# QUANTIFYING UNCERTAINTY FOR AN ELLIPTIC INVERSE PROBLEM WITH FINITE DATA

A Dissertation

by

JIAYIN LIU

Submitted to the Office of Graduate and Professional Studies of
Texas A&M University
in partial fulfillment of the requirements for the degree of

DOCTOR OF PHILOSOPHY

| | |
|---|---|
| Chair of Committee, | Michael S. Pilant |
| Committee Members, | Joseph D. Ward |
| | Peter Kuchment |
| | Michael Longnecker |
| Head of Department, | Emil Straube |

August 2015

Major Subject: Mathematics

ABSTRACT

The field of inverse problems is an area of applied mathematics that is of great importance in several scientific and industrial applications. Since an inverse problem is typically based on non-linear and ill-posed models it is often a very difficult problem to solve.

In this thesis we consider a model inverse problem in which we seek to reconstruct a coefficient in an elliptic partial differential equation from finite data. Firstly, we provide a general framework for solving such problem in Chapter 1. Then, the inverse problem is transformed into a system of ODEs by the method of characteristics. The emphasis is on the following three aspects, where new results are obtained:

a) Uniqueness of the solution of our model problem follows under some assumptions (given in Chapter 2), involving some basic concepts and using the method of characteristics. A result concerning uniqueness of the unknown parameter in the reduced model problem is proved, when the dependent variable $u$ is completely known.

b) Error estimates are derived in two dimensions using radial basis function (RBF) methods (Chapter 3, 4). An RBF inequality related to our model problem is reviewed in Chapter 3. Also an error estimate between the exact value and the approximate value of the unknown coefficient is given in Chapter 4. This inequality shows us that our parameter uncertainty is bounded by a norm in a suitable space, as well as properties of the domain and information gathered from observational data. To prove this inequality, we also derive a PDE estimate, a Sobolev embedding estimate and a RBF interpolation estimate in Chapter 4.

c) Numerical methods and reconstruction algorithms are presented (Chapter 5). We provide two different algorithms to reconstruct the unknown parameter $a$ and

multiple numerical simulations are presented in Chapter 5. Numerical results show that the error estimate $\|\tilde{a} - a\|_{L^\infty}$ and mesh norm $h$ have a linear relationship in the log-log plane. We compare the approximation results in 3 cases: $a = 1$ on the boundary $\partial\Omega$, $a = 1$ on a non-characteristic curve $\Lambda$ and asymptotic boundary condition. Numerical results show that more a priori information gives us better approximations.

# ACKNOWLEDGEMENTS

It is a great pleasure to acknowledge certain individuals that helped make this research possible.

I would like to first thank my PhD advisor, Professor Michael Pilant, for his continuous guidance, advice, understanding and support during my PH.D. To him, I own much more than I can say. I am very fortunate and pleased to work with him. In fact, this thesis would never be possible without the tremendous help he has provided.

I would also like to thank Professor Joe Ward for ideas and discussions regarding the radial basis function (RBF) method.

I am grateful for the help from Professor Peter Kuchment, whose ideas have contributed to my work.

My gratitude also goes to Professor Michael Longnecker. I thank him for taking the time to serve on both my preliminary exam committee and thesis defense committee.

The wonderful administrative staff in the Department of Mathematics, Monique Stewart, Professor Peter Howard have provided me help on various issues during my years at TAMU. I thank them for everything they have done for me and for the department, as well as my colleagues and friends for their help and support during my graduate years.

Lastly, I express all my gratitude to my parents, Xiaqiong and Peihua, for encouraging me when I was down and for being always present in my life. I dedicate this work to them.

TABLE OF CONTENTS

Page

LIST OF FIGURES

FIGURE Page

# LIST OF TABLES

TABLE Page

# 1. INTRODUCTION

A simple example of an inverse problem is to determine an unknown parameter in a model based on information we have been given through observation. There are many situations when we may not know all the parameters and they may not be easy to measure directly. These parameters frequently have to be inferred from observation of the system. But we may be able to measure some other quantities related to the parameters we are interested in. From the measurement data we have collected, we estimate the unknown parameters in the model.

Inverse problems have long been of interest in many fields of applied sciences, such as electrical impedance tomography [10], elastic imaging [5], parameter identification [26] and image processing [8].

From a mathematical point of view the goal of an inverse problem is to approximately invert a forward operator. There are three main questions that arise when we try to solve an inverse problem: existence, uniqueness and stability. In mathematics, we have a classic definition of a well-posed problem given by J. Hadamard [21]:

1. There exists a solution.

2. The solution is unique.

3. The solution is a continuous function of the data, which is also called stability.

A problem that lacks any one of these properties is called ill-posed.

Inverse problems tend to be ill-posed which means that the problem has no unique or stable solution. In other words, small changes or perturbations in measurement data can result in large differences in the corresponding solutions, for example, the reconstructed parameters.

Fortunately, many ill-posed problems can be solved in a stable manner by applying regularization. The use of regularization techniques is often necessary to solve the inverse problem in the presence of measurement noise.

After this brief introduction of the field of inverse problems, let us take a look at a particular model problem. This will also introduce the ultimate goal of our work.

## 1.1 Model problem

A model problem is formulated here for the purposes of introducing our ultimate goal. We will see how to apply characteristic methods and radial basis function (RBF) methods to such ill-posed inverse problems in the next few chapters.

In order to derive our model problem, we first consider a time-dependent diffusion problem.

Let $\Omega \in \mathbb{R}^2$ be a bounded domain and $T > 0$. We consider the following diffusion equation:

$$\begin{aligned} \frac{\partial u(x,t)}{\partial t} - \nabla \cdot (a(x)\nabla u(x,t)) &= f(x,t),\ x \in \Omega, t \in (0,T) && (1.1) \\ u(x,0) &= u_0(x),\ x \in \Omega && (1.2) \\ u(x,t) &= q(x,t),\ x \in \partial\Omega, t \in (0,T). && (1.3) \end{aligned}$$

Here $u(x,t)$ is a state variable and describes the density of a quantity at position $x$ and at time $t$. The term on the left hand describes the diffusion of $u(x,t)$, including $a(x)$ as the diffusion coefficient. The term on the right side, $f(x,t)$ is a smooth function and describes additional sources and/or sinks.

**Inverse Problem**:

Is it possible to reconstruct a good approximation to the diffusion coefficient $a(x)$

from the following set of finite measurement data?

$$u(x_i, t) = g_i(t), i = 1, 2, ...k, t \in (0, T).$$

We assume the points $x_i$ are distinct.

If we define new variables $U(x)$,$V(x)$ by

$$U(x) = \int_0^T u(x, t)dt, \tag{1.4}$$

$$F(x) = \int_0^T f(x, t)dt, \tag{1.5}$$

and integrate (1.1) over $[0, T]$, the differential equation (1.1) reduces to

$$-\nabla \cdot (a(x)\nabla U(x)) = F(x) + u_0(x) - u(x, T), x \in \Omega. \tag{1.6}$$

On the other hand, the measurement data give us:

$$U(x_i) = \int_0^T u(x_i, t)dt = \int_0^T g_i(t)dt = G_i, i = 1, 2, ...k. \tag{1.7}$$

This time-dependent problem becomes a special case of the following elliptic equation in divergence form with finite data:

Let $\Omega \in \mathbb{R}^2$ be a compact domain with smooth boundary. Given Dirichlet boundary data and interior data at prescribed points:

$$\begin{aligned} u(x_i, y_i) &= g_i, \ (x_i, y_i) \in \Omega, i = 1, 2, ...k \\ u(x, y) &= q(x, y), \ (x, y) \in \partial\Omega \end{aligned}$$

we seek to find a pair $(\tilde{a}, \tilde{u})$ with sufficient smoothness satisfying

$$\nabla \cdot (\tilde{a} \nabla \tilde{u}) = f \tag{1.8}$$

$$\tilde{u}(x_i, y_i) = g_i, \ (x_i, y_i) \in \Omega, i = 1, 2, ...k, \tag{1.9}$$

where $f$ and $g_i$ are known.

Clearly, given finite measurement data there is not a unique solution for the reconstruction, but we are interested in estimating the error of the approximation. In other words, we are interested in precisely quantifying the uncertainty. Uncertainty quantification (UQ) is a very active field of research and quantifying the uncertainty in numerical simulations is critical for successfully predicting the model response and decision-making. For example, in weather prediction, we would like to identify possible scenarios, and estimate their likelihood. Understanding and quantifying uncertainties help us to make accurate prediction for real weather activities [41]. Fields of application of uncertainty quantification include but are not limited to turbulence models [38], computational electromagnetics [9], pollutant spreading [37] and risk assessment in finance fields [11].

Uncertainties can come from variability in the environment, in the geometry (e.g., material properties), but also from boundary and initial conditions as well as parameters in the model whose exact values are unknown.

The sources of uncertainty that we consider in our model problem are parameter uncertainties which are caused by imprecise knowledge of the input data, e.g. uncertainty due to finite observational data or measurement errors. Our model parameters must be estimated from noisy and indirect observational data. Uncertainty is integral to this endeavor: observational errors, model errors, and issues of ill-posedness yield uncertainties in model parameters. This results in numerical models that are

subject to uncertainty in boundary or initial conditions as well as model parameter values. Quantifying the resulting uncertainty in parameters is then an essential part of the reconstruction process.

In Chapter 4, the main result of this thesis will be presented that an error estimate inequality between the exact value $a$ and the approximate value $\tilde{a}$ of the form

$$\|a - \tilde{a}\|_{L^\infty} \leq Ch^{\tau-4}(\|u\|_{W^{\tau,2}(\Omega)}),\ \tau > 4 \tag{1.10}$$

holds for $a$ under certain assumptions. Here $h$ is the radius of the largest inner empty disk of interpolation points. The spaces $L^\infty$ and $W^{\tau,2}$ are defined in Chapter 2.

We now consider a famous inverse conductivity problem, which is also similar to our model problem.

Let $\Omega \in \mathbb{R}^n$ be a compact domain with smooth boundary and the conductivity $\sigma : \Omega \to (0, \infty)$ is measurable, positive and bounded away from zero and infinity. Assuming there are no sources or sinks of current in $\Omega$, every voltage potential $f$ on $\partial\Omega$ induces a unique voltage potential $u$ inside $\Omega$ which satisfies the following conductivity equation:

$$\nabla \cdot (\sigma \nabla u) = 0 \ in\ \Omega \tag{1.11}$$

$$u = f\ on\ \partial\Omega. \tag{1.12}$$

The inverse conductivity problem tries to determine whether one can uniquely determine and reconstruct the conductivity $\sigma$ from full or partial knowledge of the associated Dirichlet-to-Neumann map on the boundary, i.e. the map that takes a voltage potential on the boundary (Dirichlet data) into the resulting current flux through the boundary (Neumann data):

$$\Lambda_\sigma : u \mid_{\partial\Omega} \rightarrow \sigma \frac{\partial u}{\partial \nu} \mid_{\partial\Omega}$$

Here $\nu$ is the unit outer normal to the boundary and the normal derivative on the boundary can be defined as an element of $H^{-1/2}(\partial\Omega)$ by:

$$\langle \sigma \frac{\partial u}{\partial \nu}, g \rangle = \int_\Omega \sigma \nabla u \cdot \nabla g dx \tag{1.13}$$

where $g \in H^1(\Omega)$ and $dx$ denotes the Lebesgue measure.

This inverse conductivity problem is the mathematical problem behind a method for medical imaging called Electrical Impedance Tomography (EIT) [44]. One of the important early papers on the inverse conductivity problem was authored by A.P. Calderón [7] in 1980. He showed the injectivity of a linearized problem near $\sigma \equiv 1$. Other more recent papers solve the inverse conductivity problem in dimension two with various assumptions, such as Kohn and Vogelius [27] [28], Alessandrini [2] [3], Nachman [32] and finally Astala and Päivärinta [4]. Kohn and Vogelius solved the uniqueness question for the class of real-analytic conductivities [27], a result that was later generalized to piecewise real-analytic conductivity [28]. Stability results were obtained by Alessandrini in [2] and [3]. Nachman converted the conductivity equation into the Schrödringer equation and proved uniqueness for $\sigma \in W^{2,p}, p > 1$ . The paper of Astala and Päivärinta solved the inverse conductivity problem most generally: there were no requirements on the smoothness of the conductivity. It must be positive and bounded away from zero and infinity, which is physically realistic.

There are similarities between the inverse conductivity problem and our model problem. They both seek to recover the coefficient from an elliptic equation. The major difference between them is the amount of data used to recover the coefficient. The inverse conductivity problem uses complete information on the boundary but our model problem has only finite interior data. There are results for the inverse

conductivity with Dirichlet-Neumann as well as interior data, see [29], [30].

## 1.2 Contents of the thesis

The thesis is divided into 6 chapters. In Chapter 2, we introduce some basic concepts regarding Sobolev spaces and the method of characteristics. Then we will use this method to prove the uniqueness of the solution of the unknown model problem under some assumptions. Based on the paper in Narcowich, Ward and Wendland [35], a short review of an RBF inequality related to our model equation is analyzed in Chapter 3. In Chapter 4, we derive an error estimate inequality to compare between the exact value and the approximated value. We propose a numerical algorithm to reconstruct the unknown variable $a$ in Chapter 5. A number of simulations are also considered. In Chapter 6 conclusions are presented.

# 2. MODEL PROBLEM

In this chapter we will first introduce the concepts related to Sobolev spaces, Hölder spaces and the method of characteristics. After that, we will apply the method of characteristics to our model problem. Then a result concerning existence and uniqueness of the solution of a reduced model problem is proved.

## 2.1 Mathematical preliminaries

In this section we present the necessary theoretical background to this thesis. We give a brief overview of Sobolev spaces and their norms. Afterwards we define Hölder spaces and norms. Finally, we recall basic properties of method of characteristics that will be helpful in the following section where we prove the existence and uniqueness of the solution of a reduced model problem.

### *2.1.1 Sobolev spaces*

Throughout this thesis Sobolev spaces and norms will play an important role. Consequently, we briefly summerize the definition of a Sobolev space and its norm in the following:

**Definition 2.1.1** ($L^p$ norm, [14])**.** For $1 \leq p < \infty$,

$$\|u\|_{L^p} = \left( \int |u|^p \right)^{\frac{1}{p}} \tag{2.1}$$

**Definition 2.1.2** ($L^p(\Omega)$ space, [14])**.** For $1 \leq p < \infty$,

$$L^p(\Omega) = \{u : \Omega \to \mathbb{R} \mid u \textit{ is Lebesgue measurable}, \ \|u\|_{L^p(\Omega)} < \infty\}. \tag{2.2}$$

**Definition 2.1.3** ($L^\infty$ norm and space, [14])**.**

$$L^\infty(\Omega) = \{u : \Omega \to \mathbb{R} \mid u \text{ is Lebesgue measurable}, \ \|u\|_{L^\infty(\Omega)} < \infty\} \tag{2.3}$$

where

$$\|u\|_{L^\infty(\Omega)} = ess\ sup_\Omega |u|.$$

**Definition 2.1.4** (Multi-index notation, [14])**.** A vector of the form $\alpha = (\alpha_1, ..., \alpha_n)$, where each component $\alpha_i$ is a non-negative integer , is called a multi-index of order:

$$|\alpha| = |\alpha_1| + |\alpha_2| + \cdots + |\alpha_n|.$$

Assume $u : U \to \mathbb{R}$,$x \in U$, given a multi-index $\alpha$ define:

$$D^\alpha u(x) = \frac{\partial^{|\alpha|} u(x)}{\partial x_1^{\alpha_1} \cdots \partial x_n^{\alpha_n}}.$$

**Definition 2.1.5** (Sobolev Norm, [14])**.** For $n \in \mathbb{N}, k > 0$ and $1 \leq p < \infty$,

$$\|u\|_{k,p} = \left( \sum_{0 \leq |\alpha| \leq k} \|D^\alpha u\|_p^p \right)^{\frac{1}{p}} \tag{2.4}$$

After introducing the Sobolev norm and multi-index notation, we recall the definition of Sobolev spaces, which is related to the Sobolev norm. To understand this concept, we also give the definition of weak derivatives.

**Definition 2.1.6** (Weak derivatives, [14])**.** Suppose $u, v \in L^1_{loc}(\Omega)$, and $\alpha$ is a Multi-index. We say that $v$ is a $\alpha^{th}$-weak partial derivative of $u$, written

$$D^\alpha u = v,$$

provided

$$\int_\Omega uD^\alpha \phi dx = (-1)^{|\alpha|} \int_\Omega v\phi dx. \tag{2.5}$$

for all test functions $\phi \in C_c^\infty(\Omega)$. ($C_c^\infty(\Omega)$ denotes the space of functions in $C^\infty(\Omega)$ with compact support.)

**Definition 2.1.7** (Sobolev Spaces, [14])**.** For $k > 0$ and $1 \leq p < \infty$, the Sobolev space

$$W^{k,p}(\Omega)$$

consists of all locally summable functions $u : \Omega \to \mathbb{R}$ such that for each multi-index $\alpha$ with $|\alpha| \leq k$, $D^\alpha u$ exists in the weak sense and belongs to $L^p(\Omega)$.

Usually, we write $H^k(\Omega) = W^{k,2}(\Omega)$. After all the introductions about the integer valued Sobolev spaces, we would like to give some definitions about the fractional Sobolev spaces and norms.

**Definition 2.1.8** (Fractional Sobolev spaces, [36])**.** Let $\Omega$ be a domain in $\mathbb{R}^n$, $s \in (0, 1)$. For any $p \in [1, \infty)$, we define $W^{s,p}(\Omega)$ as follows:

$$W^{s,p}(\Omega) = \left\{ u \in L^p(\Omega) : \frac{|u(x) - u(y)|}{|x - y|^{\frac{n}{p}+s}} \in L^p(\Omega \times \Omega) \right\}. \tag{2.6}$$

i.e, an intermediary Banach space between $L^p(\Omega)$ and $W^{1,p}(\Omega)$.

**Definition 2.1.9** (Fractional Sobolev norm, [36])**.** Let $\Omega$ be a domain in $\mathbb{R}^n$, $s \in (0, 1)$. For any $p \in [1, \infty)$,

$$\|u\|_{W^{s,p}(\Omega)} := \left( \int_\Omega |u|^p \, dx + \int_\Omega \int_\Omega \frac{|u(x) - u(y)|^p}{|x - y|^{n+sp}} \, dxdy \right)^{\frac{1}{p}} \tag{2.7}$$

where the second term in (2.7)

$$|u|_{W^{s,p}(\Omega)} := \left( \int_\Omega \int_\Omega \frac{|u(x) - u(y)|^p}{|x-y|^{n+sp}} \, dxdy \right)^{\frac{1}{p}} \tag{2.8}$$

is also called Gagliardo seminorm of $u$.

### *2.1.2 Hölder spaces*

We state in this section the definitions and results we shall need from the theory of Hölder spaces.

**Definition 2.1.10** (Hölder Seminorm, [14])**.** Let $\Omega$ be a open subset in $\mathbb{R}^d$. If $\mu \in (0, 1]$, the usual Hölder seminorm is given by

$$[f]_{0,\mu;\Omega} = \sup_{x,y\in\Omega} \frac{|f(x) - f(y)|}{|x-y|^\mu}. \tag{2.9}$$

**Definition 2.1.11** (Hölder Space, [14])**.** The class of $f \in C(\Omega)$ such that $[f]_{0,\mu;\Omega} < \infty$ will be denoted as the Hölder space $C^{0,\mu}(\Omega)$. Functions in $C^{0,\mu}(\Omega)$ are said to be uniformly Hölder continuous with exponent $\mu$.

**Definition 2.1.12** (Hölder Norm, [14])**.** The full Hölder norm of $f$ is defined as follows:

$$\|f\|_{0,\mu;\Omega} = \sup_{x\in\Omega} |f(x)| + [f]_{0,\mu;\Omega}. \tag{2.10}$$

We may also define spaces of continuously differentiable functions whose $kth$ derivative is Hölder continuous.

**Definition 2.1.13.** For any integer $k \geq 0$, we let $C^{k,\mu}(\Omega)$ denote the set of all functions in $f \in C^k(\Omega)$ with $D^\beta f \in C^{0,\mu}(\Omega)$ for each multi-index $\beta$ with $|\beta| = k$.

For $f \in C^{k,\mu}(\Omega)$, we define the semi-norm:

$$[f]_{k,\mu;\Omega} = \sum_{|\beta|=k} \sup_{x,y\in\Omega} \frac{|D^\beta f(x) - D^\beta f(y)|}{|x-y|^\mu}. \tag{2.11}$$

The appropriate full norm is given by

$$\|f\|_{k,\mu;\Omega} = \sum_{|\beta|\leq k} \sup_{x\in\Omega} |D^\beta f(x)| + [f]_{k,\mu;\Omega} \tag{2.12}$$

where $\beta$ ranges over all multi-indices of appropriate orders.

### *2.1.3 Sobolev embedding theorems*

In this section we summarize the Sobolev Embedding Theorems. We start by considering continuous, compact, and bounded operators first, and then provide Sobolev Embedding Theorems for both integer and fractional Sobolev spaces.

**Definition 2.1.14** (Operators, [1])**.** Let $X$, $Y$ be normed spaces and $f$ an operator from $X$ into $Y$.

1. $f$ is continuous if and only if $f(x_n) \to f(x)$ in $Y$ whenever $x_n \to x$ in $X$.
2. $f$ is compact if $f(A)$ is precompact in $Y$ whenever $A$ is bounded in $X$.
3. $f$ is bounded if $f(A)$ is bounded in $Y$ whenever $A$ is bounded in $X$.
4. $f$ is completely continuous if it is continuous and compact.

**Definition 2.1.15** (Embeddings, [1])**.** The normed space $X$ is embedded in the normed space $Y$, denoted by $X \to Y$ if:

1. $X$ is a vector subspace of $Y$ and

2. the identity operator $I$ defined on $X$ into $Y$ by $Ix = x$ for all $x \in X$ is continuous.

$X$ is compactly embedded in $Y$ if the embedding operator $I$ is compact.

The next statement is Sobolev embedding theorem. It is an important result when proving the error estimates in chapter 4.

**Theorem 2.1.1** (Sobolev Embedding Theorem, [1]). *Let $\Omega$ be a bounded domain in $\mathbb{R}^n$ with Lipschitz boundary. Let $k \geq 1$ and let $1 \leq p \leq \infty$.*

1. *If either $k > l$ and $1 \leq p \leq q \leq \infty$ are two extended real numbers such that*

$$\frac{1}{q} = \frac{1}{p} - \frac{k-l}{n} \tag{2.13}$$

*then*

$$W^{k,p}(\Omega) \subseteq W^{l,q}(\Omega). \tag{2.14}$$

2. *If $(k - r - \alpha)/n = 1/p$ with $\alpha \in (0, 1)$, then*

$$W^{k,p}(\Omega) \subset C^{r,\alpha}(\Omega). \tag{2.15}$$

3. *If $k > \frac{n}{p} + 1$, then*

$$W^{k,p}(\Omega) \subset C^{0,1}(\Omega). \tag{2.16}$$

In addition, we have several embedding theorems for fractional Sobolev spaces. Before we state the embedding theorems, we need the following definition as a constraint for the domain.

**Definition 2.1.16** (Extension domain, [36]). For any $s \in (0, 1)$, and any $p \in [1, \infty)$, we say that an open set $\Omega \in \mathbb{R}^n$ is an extension domain for $W^{s,p}$, if there exists a

positive constant $C = C(n, p, s, \Omega)$ such that: for every function $u \in W^{s,p}(\Omega)$, there exists $\tilde{u} \in W^{s,p}(\mathbb{R}^n)$ with $\tilde{u}(x) = u(x)$ for all $x \in \Omega$ and $\|\tilde{u}\|_{W^{s,p}(\mathbb{R}^n)} \leq C\|u\|_{W^{s,p}(\Omega)}$.

**Theorem 2.1.2** (Theorem 5.4, [36]). *Let $s \in (0,1)$ and $p \in [1,\infty)$ and $\Omega \subseteq \mathbb{R}^n$ be an open set of class $C^{0,1}$ with bounded boundary (Lipschitz domain). Then $W^{s,p}(\Omega)$ is continuously embedded in $W^{s,p}(\mathbb{R}^n)$, namely for any $u \in W^{s,p}(\Omega)$, there exists $\tilde{u} \in W^{s,p}(\mathbb{R}^n)$ such that $\tilde{u}\big|_{\Omega} = u$, and*

$$\|\tilde{u}\|_{W^{s,p}(\mathbb{R}^n)} \leq C\|u\|_{W^{s,p}(\Omega)} \tag{2.17}$$

*where $C = C(n, p, s, \Omega)$.*

**Theorem 2.1.3** (Theorem 6.7, [36]). *Let $s \in (0,1)$ and $p \in [1,\infty)$, such that $sp < n$. Let $\Omega \subseteq \mathbb{R}^n$ be a bounded extension domain for $W^{s,p}$. Then there exists a positive constant $C = C(n, p, s, \Omega)$ such that for any $f \in W^{s,p}(\Omega)$, we have*

$$\|f\|_{L^q(\Omega)} \leq C\|f\|_{W^{s,p}(\Omega)} \tag{2.18}$$

*where $q \in [p, p^\star := \frac{np}{n-sp}]$.*

**Theorem 2.1.4** (Theorem 6.10, [36]). *Let $s \in (0,1)$ and $p \in [1,\infty)$, such that $sp = n$. Let $\Omega \subseteq \mathbb{R}^n$ be a bounded extension domain for $W^{s,p}$. Then there exists a positive constant $C = C(n, p, s, \Omega)$ such that for any $f \in W^{s,p}(\Omega)$, we have*

$$\|f\|_{L^q(\Omega)} \leq C\|f\|_{W^{s,p}(\Omega)} \tag{2.19}$$

*where $q \in [p, \infty)$.*

**Theorem 2.1.5** (Theorem 7.1, [36]). *Let $s \in (0,1)$ and $p \in [1,\infty)$. Let $q \in [1, p]$, $\Omega \subseteq \mathbb{R}^n$ be a bounded extension domain for $W^{s,p}$ and $\mathcal{I}$ be a bounded subset of $L^p(\Omega)$.*

*Suppose that*

$$\sup_{f\in\mathcal{I}}\int_\Omega\int_\Omega \frac{|f(x)-f(y)|^p}{|x-y|^{n+sp}}\,dxdy<\infty.$$

*Then $\mathcal{I}$ is pre-compact in $L^q(\Omega)$.*

**Theorem 2.1.6** (Corollary 7.2, [36]). *Let $s\in(0,1)$ and $p\in[1,\infty)$ such that $sp<n$. Let $q\in[1,p^\star=\frac{np}{n-sp})$, $\Omega\subseteq\mathbb{R}^n$ be a bounded extension domain for $W^{s,p}$ and $\mathcal{I}$ be a bounded subset of $L^p(\Omega)$. Suppose that*

$$\sup_{f\in\mathcal{I}}\int_\Omega\int_\Omega \frac{|f(x)-f(y)|^p}{|x-y|^{n+sp}}\,dxdy<\infty.$$

*Then $\mathcal{I}$ is pre-compact in $L^q(\Omega)$.*

**Theorem 2.1.7** (Theorem 8.2, [36]). *Let $s\in(0,1)$ and $p\in[1,\infty)$ such that $sp>n$. Let $\Omega\subseteq\mathbb{R}^n$ be a Lipschitz domain for $W^{s,p}$. Then there exists $C>0$, depending on $n,s,p$ and $\Omega$, such that*

$$\|f\|_{C^{0,\alpha}(\Omega)}\leq C\|f\|_{W^{s,p}(\Omega)} \tag{2.20}$$

*for any $f\in W^{s,p}$, with $\alpha:=\frac{sp-n}{p}$.*

*In addition, for any $q\in[1,\infty)$, there exists $C_2>0$ that*

$$\|f\|_{L^q(\Omega)}\leq C_2\|f\|_{W^{s,p}(\Omega)} \tag{2.21}$$

*for any $f\in W^{s,p}$.*

Taking into account the previous theorems, we are able to give the General Sobolev inequalities stated in the following theorem.

**Theorem 2.1.8** (General Sobolev inequalities, [14]). *Let $\Omega$ be a bounded open subset of $R^n$, with a $C^1$ boundary. Assume $u\in W^{k,p}(\Omega)$.*

*(i) If $k < \frac{n}{p}$, then $u \in L^q(\Omega)$, where $\frac{1}{q} = \frac{1}{p} - \frac{k}{n}$. We have in addition the estimate:*

$$\|u\|_{L^q(\Omega)} \leq C\|u\|_{W^{k,p}(\Omega)} \tag{2.22}$$

*the constant $C$ depending only on $k, p, n$ and $\Omega$.*

*(ii) If $k > \frac{n}{p}$, then $u \in C^{k-[\frac{n}{p}]-1,\mu}(\Omega)$, where $\mu = [\frac{n}{p}] + 1 - \frac{n}{p}$ if $\frac{n}{p}$ is not an integer, or $\mu$ is any positive number $< 1$, if $\frac{n}{p}$ is an integer. We have in addition the estimate:*

$$\|u\|_{C^{k-[\frac{n}{p}]-1,\mu}(\Omega)} \leq C\|u\|_{W^{k,p}(\Omega)} \tag{2.23}$$

*the constant $C$ depending only on $k, p, n, \mu$ and $\Omega$. (Note: $[x]$ defines the nearest integer to $x$.)*

### *2.1.4 Method of characteristics*

First-order partial differential equations can be reformulated as systems of ordinary differential equations along characteristic curves or characteristics. We will briefly discuss the method in this section and apply it to our work in the next section.

Consider the first-order, nonlinear equation,

$$F(\vec{x}, u, Du) = 0, \quad \vec{x} \in \mathbb{R}^n \text{ in } U, \tag{2.24}$$

subject to the boundary condition:

$$u = g \text{ on } \Gamma \tag{2.25}$$

where $\Gamma \subseteq \partial U$ and $g : \Gamma \to \mathbb{R}$ are given. We also suppose that $F$, $g$ are continuous.

First, we parameterize $\Gamma$ by the vector $\vec{r} = (r_1, r_2, ..., r_{n-1}) \in \mathbb{R}^{n-1}$, so that $\Gamma = (\gamma_1(\vec{r}), \gamma_2(\vec{r}), ..., \gamma_n(\vec{r}))$. We also define $z(s) = u(\vec{x}(s))$ and $\vec{p}(s) = Du(\vec{x}(s))$,

that is, $\vec{p}(s) = (p_1(s), p_2(s), ..., p_n(s))$, where $p_i(s) = u_{x_i}(\vec{x}(s))$.

We rewrite our equation as

$$F(\vec{x}, z, \vec{p}) = 0.$$

**Definition 2.1.17** (Evans, [14])**.** We define $2n+1$ *characteristic equations* by:

$$\begin{aligned} \frac{dx_i}{ds} &= F_{p_i}. \\ \frac{dz}{ds} &= \sum_{i=1}^{n} p_i F_{p_i}. \\ \frac{dp_i}{ds} &= -F_{x_i} - F_z p_i. \end{aligned} \tag{2.26}$$

for $i = 1, 2, ..., n$. The functions $\vec{x}(s)$,$z(s)$ and $\vec{p}(s)$ are called the *characteristics*. The graph of the solution to this system of ODEs must be a union of integral curves. These integral curves are called the *characteristic curves* of the original partial differential equation.

For $i = 1, 2, ..., n$, we give the initial conditions as follows:

$$\begin{aligned} x_i(\vec{r}, 0) &= \gamma_i(\vec{r}). \\ z(\vec{r}, 0) &= g(\vec{r}). \\ p_i(\vec{r}, 0) &= h_i(\vec{r}). \end{aligned} \tag{2.27}$$

where the functions $h_i$, $i = 1, 2, ..., n$ satisfy the following *compatibility conditions*:

$$\begin{aligned} &F(\gamma_1(\vec{r}), ...\gamma_1(\vec{r}), g(\vec{r}), h_1(\vec{r}), ...h_1(\vec{r})) = 0. \\ &g_{r_i} = h_1(\vec{r})\frac{\partial \gamma_1}{\partial r_i} + \cdots + h_n(\vec{r})\frac{\partial \gamma_n}{\partial r_i}, \quad i = 1, 2, ...n-1. \end{aligned} \tag{2.28}$$

Note $z(\vec{r}, 0)$ is uniquely determined by the boundary condition and the choice of point $\vec{x}(\vec{r}, 0)$, but the vector function $\vec{h}$ satisfying (2.28) may not exist or may not

be unique. But if they do exist, we are able to find a unique solution to this system from ODE theory.

In order to guarantee that we can invert the function $z(\vec{r}, s)$ to the function $u(\vec{x})$, we require an additional boundary condition near $\Gamma$:

**Definition 2.1.18** (Noncharacteristic Boundary Condition, [14])**.** We denote $h(\vec{r}) = (h_1(\vec{r}), h_2(\vec{r}), ...h_n(\vec{r}))$ and say $(\Gamma(\vec{r}), g(\vec{r}), h(\vec{r}))$ is *noncharacteristic* if

$$D_{\vec{p}}(\Gamma(\vec{r}), g(\vec{r}), h(\vec{r})) \cdot \nu(\Gamma(\vec{r})) \neq 0 \tag{2.29}$$

where $\nu(\Gamma(\vec{r}))$ denotes the outward unit normal to $\partial U$ at $\Gamma(\vec{r})$.

Then, we have the following Lemma:

**Lemma 2.1.9.** *If $\Gamma$ is noncharacteristic (2.29), then there exists an open interval $I \subset \mathbb{R}$ containing $0$, a neighborhood $W$ of $\vec{r} = \vec{x}(r_1, r_2, ..., r_{n-1})$ in $\Gamma \subset \mathbb{R}^{n-1}$, and a neighborhood $V$ of $h(\vec{r}) = (h_1(\vec{r}), h_2(\vec{r}), ...h_n(\vec{r}))$ in $\mathbb{R}^n$, such that for each $x \in V$ there exists unique $s \in I$, $y \in W$ such that*

$$x = G(s, y). \tag{2.30}$$

*Proof.* The key ingredient used in the proof is Inverse Function Theorem. The proof of this lemma can be found in Evans [14] and is omitted here.

The technique of reducing a partial differential equation to a system of ordinary differential equations by introducing these characteristic equations is called *the method of characteristics*. Now we will proceed to solve equation (1.8) for our model problem, using the method of characteristics.

## 2.2 Reduction to a first order system of ODEs

In this section we reduce our model problem to a system of ODEs.

At first, We give some assumptions to our problem as follows:

**Assumption 2.2.1.**

- *Existence: there is a smooth solution $u$ of $\nabla \cdot (a\nabla u) = f$, given $f$ and $a$ sufficiently smooth.*
- *Uniform ellipticity: there exists a constant $c > 0$, such that $c^{-1} \leq a(x, y) \leq c$.*
- *No interior extrema: $|\nabla u| \geq \delta > 0$.*
- *Noncharacteristic boundary condition. See Definition 2.1.18.*

Note that the first item of the previous assumptions implies that (1.8) admits a solution in $H^k(\Omega)$ for some $k$ (see [14]). We will later use this regularity result. The second item ensures the positivity of $a$ and the third item is the consequence of the maximum principle for (1.8). We state last item more precisely as follows. For each $r \in \mathbb{R}$ and $(\gamma_1(r), \gamma_2(r)) \in \partial\Omega$,

$$\frac{\partial u}{\partial \gamma_1} \cdot \gamma_2'(r) - \frac{\partial u}{\partial \gamma_2} \cdot \gamma_1'(r) \neq 0. \tag{2.31}$$

This result comes from the definition of noncharacteristic boundary condition in last section.

To guarantee that our approximation $a$ will be positive, we simplify our problem by making the transformation $a(x, y) = e^{\phi(x,y)}$. Equation (1.8) then becomes:

$$e^{\phi} \cdot (\nabla\phi \cdot \nabla u + \nabla^2 u) = f \tag{2.32}$$

which yields:

$$F(\vec{x}, \phi, D\phi) = \nabla\phi \cdot \frac{\nabla u}{|\nabla u|} + \frac{\nabla^2 u}{|\nabla u|} - \frac{e^{-\phi} \cdot f}{|\nabla u|} = 0. \tag{2.33}$$

A solution $\phi(x(s), y(s)) := z(s)$ parameterized by arc length $s$ has to satisfy:

$$\frac{dz}{ds} = \frac{d}{ds}\phi(x, y) = \frac{\partial\phi}{\partial x} \cdot \frac{dx}{ds} + \frac{\partial\phi}{\partial y} \cdot \frac{dy}{ds}. \tag{2.34}$$

Comparison with (2.33) suggests setting $\frac{dx}{ds} = \frac{u_x}{|\nabla u|}$ and $\frac{dy}{ds} = \frac{u_y}{|\nabla u|}$, so that:

$$\frac{dz}{ds} = \frac{\partial\phi}{\partial x} \cdot \frac{u_x}{|\nabla u|} + \frac{\partial\phi}{\partial y} \cdot \frac{u_y}{|\nabla u|} = -\frac{\nabla^2 u}{|\nabla u|} + \frac{e^{-\phi} \cdot f}{|\nabla u|}. \tag{2.35}$$

Therefore, the PDE has been transformed to the system of ODEs along the characteristic curves:

$$\begin{aligned} \frac{d\phi}{ds} &= -\frac{\nabla^2 u}{|\nabla u|} + \frac{e^{-\phi} \cdot f}{|\nabla u|}. \\ \frac{dx}{ds} &= \frac{u_x}{|\nabla u|}. \\ \frac{dy}{ds} &= \frac{u_y}{|\nabla u|}. \end{aligned} \tag{2.36}$$

For convenience, we also assume that $a = 1$ on the boundary, which implies that $\phi = 0$ on the boundary.

We will use equations (2.36) to reconstruct the unknown conductivity $a(x, y)$ from $u(x, y)$.

## 2.3 Existence and uniqueness of solutions with known function $u$

In this section, our model problem is reduced to a problem where $u$ is completely known. We derive a result concerning existence and uniqueness for the reduced model problem.

After introducing the method of characteristics, we now have the tools to demonstrate the local existence and uniqueness of the reduced model problem.

Applying the definitions from Section 2.1.4 to our equation (2.33), we define $\vec{x}(s) = (x(s), y(s))$, $z(s) = \phi(x(s), y(s))$ and $\vec{p}(s) = D\phi(x(s), y(s))$. We also parameterize $\partial\Omega$ by $r$, so that $\partial\Omega = (\gamma_1(r), \gamma_2(r))$. Our equation (2.33) has the new form:

$$F(\vec{x}, z, \vec{p}) = \vec{p}(s) \cdot \frac{\nabla u}{|\nabla u|} + \frac{\nabla^2 u}{|\nabla u|} - \frac{e^{-z(s)} \cdot f}{|\nabla u|} = 0. \tag{2.37}$$

We define 5 characteristic equations by

$$\begin{aligned} \frac{dz}{ds} &= F_{\vec{p}} = -\frac{\nabla^2 u}{|\nabla u|} + \frac{e^{-z} \cdot f}{|\nabla u|}. \\ \frac{d\vec{x}}{ds} &= \vec{p} \cdot F_{\vec{p}} = \frac{\nabla u}{|\nabla u|}. \\ \frac{d\vec{p}}{ds} &= -F_{\vec{x}} - F_z \cdot \vec{p} = -F_{\vec{x}} + \frac{e^{-z} \cdot f}{|\nabla u|}\vec{p}. \end{aligned} \tag{2.38}$$

Initial conditions are given as follows:

$$\begin{aligned} &\vec{x}(r, 0) = (\gamma_1(r), \gamma_2(r)). \\ &z(r, 0) = 0. \\ &\vec{p}(r, 0) = (h_1(r), h_2(r)). \end{aligned} \tag{2.39}$$

To prove the local existence and uniqueness of the solution of the reduced model problem, we start with several lemmas. First of all, we prove the following lemma:

**Lemma 2.3.1.** *For any point $(\gamma_1(r_0), \gamma_2(r_0)) \in \partial\Omega$, there exists a unique solution $(h_1(r), h_2(r))$ of equation (2.28) for all $r \in \partial\Omega$ sufficiently close to $r_0$ such that the solution satisfies compatibility conditions.*

*Proof.* According to (2.28), $(h_1(r), h_2(r))$ satisfies the following system of linear equa-

tions:

$$\begin{aligned} f(\gamma_1(r),\gamma_2(r)) - \nabla^2 u(\gamma_1(r),\gamma_2(r)) &= \frac{\partial u(\gamma_1,\gamma_2)}{\partial \gamma_1} h_1(r) + \frac{\partial u(\gamma_1,\gamma_2)}{\partial \gamma_2} h_2(r). \\ 0 &= \frac{d\gamma_1(r)}{dr} h_1(r) + \frac{d\gamma_2(r)}{dr} h_2(r). \end{aligned} \tag{2.40}$$

Recall from our assumption that $\partial\Omega$ is noncharacteristic. By (2.31), we have

$$\begin{vmatrix} \frac{\partial u}{\partial \gamma_1} & \frac{\partial u}{\partial \gamma_2} \\ \frac{d\gamma_1(r)}{dr} & \frac{d\gamma_2(r)}{dr} \end{vmatrix} = \frac{\partial u}{\partial \gamma_1} \cdot \gamma_2'(r) - \frac{\partial u}{\partial \gamma_2} \cdot \gamma_1'(r) \neq 0.$$

Therefore, this system of linear equation has unique solution for $(h_1(r), h_2(r))$.

Consequently, Lemma 2.3.1 guarantees compatibility condition on the boundary. The next lemma is about existence and uniqueness of the solution of the system of ODEs. We omit the proof since it is a direct application of ODE Existence Theorem [45].

**Lemma 2.3.2.** *There is a unique local solution to the characteristic equations* (2.38) *with initial conditions* (2.39)*.*

*Remark*: We need Lipschitz continuity of $\nabla^2 u$ to prove the uniqueness of the solution.

The following lemma describes the local invertibility from $(r, s)$ to $(x, y)$.

**Lemma 2.3.3.** *For each $r_0$, there exists an open set $V$ containing the point $(r_0, 0)$ and an open set $W$ containing the point $G(r_0, 0) = (x(r_0, 0), y(r_0, 0)) = (\gamma_1(r_0), \gamma_2(r_0))$, such that*

$$G : V \to W$$

*is one-to-one and onto, and the inverse function*

$$G^{-1} : W \to V$$

*is* $C^1$.

*Proof.* This is a straightforward consequence of Lemma 2.1.9.

We have all the lemmas we need to prove the local existence and uniqueness of the solution of the reduced model problem, so let us state the theorem.

**Theorem 2.3.4.** *For any point* $(\gamma_1(r_0), \gamma_2(r_0)) \in \partial\Omega$*, there exists a unique solution of* (2.33) *with boundary condition* $\phi = 0$ *on* $\partial\Omega$ *in some neighborhood* $V$ *containing* $(\gamma_1(r_0), \gamma_2(r_0))$.

*Proof.* According to Lemma 2.3.2, let $(\vec{x}(r,s), z(r,s), \vec{p}(r,s))$ be the unique local solution of (2.38), (2.39) in a neighborhood $V$ of $(\gamma_1(r_0), \gamma_2(r_0))$. We can invert the function $\vec{x}(r,s)$ in some neighborhood near $(\gamma_1(r_0), \gamma_2(r_0))$ by Lemma 2.3.3. We assume without loss of generality that this neighborhood is also $V$. To be more precisely, we can find functions $r$,$s$ such that $r = r(\vec{x})$,$s = s(\vec{x})$ in $V$.

Now, let us define

$$\phi(\vec{x}) \equiv \phi(x,y) \equiv z(r,s) = z(r(\vec{x}), s(\vec{x}))$$

for every point $x \in V$.

We assert that this function $\phi$ solves our model PDE (2.33) with boundary condition $\phi = 0$. In order to prove this, first of all, let us demonstrate that

$$F(\vec{x}(r,s), z(r,s), \vec{p}(r,s)) = 0. \tag{2.41}$$

To see this, note

$$F(\vec{x}(r,0), z(r,0), \vec{p}(r,0)) = 0 \tag{2.42}$$

by the compatibility conditions (2.28). Moreover, we have

$$\begin{aligned}\frac{\partial F}{\partial s}(\vec{x},z,\vec{p}) &= \frac{\partial F}{\partial \vec{x}}\frac{\partial \vec{x}}{\partial s}+\frac{\partial F}{\partial z}\frac{\partial z}{\partial s}+\frac{\partial F}{\partial \vec{p}}\frac{\partial \vec{p}}{\partial s}\\ &= F_{\vec{x}}\cdot F_{\vec{p}}+F_z\cdot(\vec{p}\cdot F_{\vec{p}})+F_{\vec{p}}\cdot(-F_{\vec{x}}-F_z\cdot\vec{p}) \quad (By\ (2.38)\ )\\ &= 0.\end{aligned}$$

This result and (2.42) lead to (2.41). In view of definition of $\phi$ and (2.41), we can conclude that

$$F(\vec{x},\phi,\vec{p})=0. \tag{2.43}$$

It remains to prove:

$$\vec{p}=D\phi. \tag{2.44}$$

In order to show this, we need following two identities:

$$\frac{\partial z}{\partial s}(r,s)=\vec{p}\cdot\frac{\partial \vec{x}}{\partial s} \tag{2.45}$$

and

$$\frac{\partial z}{\partial r}(r,s)=\vec{p}\cdot\frac{\partial \vec{x}}{\partial r}. \tag{2.46}$$

These two identities will help us prove (2.44). We obtain our first identity using characteristic equations (2.38). To establish second identity, we fix $r$ and set:

$$L(s)=\frac{\partial z}{\partial r}(r,s)-\vec{p}\cdot\frac{\partial \vec{x}}{\partial r}(r,s). \tag{2.47}$$

It is easy to check that $L(0)=0$ according to the compatibility conditions (2.28). In

addition, we can compute:

$$\begin{aligned} L'(s) &= \frac{\partial^2 z}{\partial r \partial s} - (\frac{\partial \vec{p}}{\partial s}\frac{\partial \vec{x}}{\partial r} + \vec{p}\cdot\frac{\partial^2 \vec{x}}{\partial r \partial s}) && (2.48)\\ &= (\frac{\partial \vec{p}}{\partial r}\frac{\partial \vec{x}}{\partial s} + \vec{p}\cdot\frac{\partial^2 \vec{x}}{\partial s \partial r}) - (\frac{\partial \vec{p}}{\partial s}\frac{\partial \vec{x}}{\partial r} + \vec{p}\cdot\frac{\partial^2 \vec{x}}{\partial r \partial s}) \quad (By\ (2.45)\ ) && (2.49)\\ &= \frac{\partial \vec{p}}{\partial r}\frac{\partial \vec{x}}{\partial s} - \frac{\partial \vec{p}}{\partial s}\frac{\partial \vec{x}}{\partial r} && (2.50)\\ &= \frac{\partial \vec{p}}{\partial r}\cdot F_{\vec{p}} + (F_{\vec{x}} + F_z\cdot\vec{p})\frac{\partial \vec{x}}{\partial r}.\quad (By\ (2.38)\ ) && (2.51) \end{aligned}$$

Now differentiate (2.41) with respect to $r$:

$$F_{\vec{x}}\cdot\frac{\partial \vec{x}}{\partial r} + F_z\cdot\frac{\partial z}{\partial r} + F_{\vec{p}}\cdot\frac{\partial \vec{p}}{\partial r} = 0. \tag{2.52}$$

We employ this identity in (2.48), obtaining:

$$L'(s) = F_z\cdot(\vec{p}\cdot\frac{\partial \vec{x}}{\partial r} - \frac{\partial z}{\partial r}) = -F_z L(s). \tag{2.53}$$

Note that $F$ is Lipschitz continuous with respect to $z$. Hence $L(s)$ solves the linear ODE (2.53), with the initial condition $L(0) = 0$. Consequently, $L(s) = 0$ and so identity (2.46) is verified.

We finally employ (2.45) and (2.46) in proving (2.44). Indeed,

$$\begin{aligned} \frac{\partial \phi}{\partial \vec{x}} &= \frac{\partial z}{\partial s}\frac{\partial s}{\partial \vec{x}} + \frac{\partial z}{\partial r}\frac{\partial r}{\partial \vec{x}}\\ &= (\vec{p}\cdot\frac{\partial \vec{x}}{\partial s})\frac{\partial s}{\partial \vec{x}} + (\vec{p}\cdot\frac{\partial \vec{x}}{\partial r})\frac{\partial r}{\partial \vec{x}} \quad (By\ (2.45),\ (2.46)\ )\\ &= \vec{p}\cdot(\frac{\partial \vec{x}}{\partial s}\frac{\partial s}{\partial \vec{x}} + \frac{\partial \vec{x}}{\partial r}\frac{\partial r}{\partial \vec{x}})\\ &= \vec{p}. \end{aligned}$$

This concludes the proof of (2.44), and so completes the proof of existence of the

solution.

Uniqueness of the solution is guaranteed due to uniqueness theorem for ODEs and uniqueness of local invertibility.

*Remark:* Although we have utilized the full characteristic equations (2.38) in the proof of Theorem 2.3.4, once we know the solution exists, we can use some of equations (2.36) (which do not involve $\vec{p}(\cdot)$ to compute the solution. Observe also the characteristics $x(s)$ emanating from distinct points on $\partial\Omega$ cannot cross, owing to uniqueness of solutions of the initial-valued problem for the ODE.

**Corollary 2.3.5.** *For any point $(x_0, y_0) \in \partial\Omega$, there exists a unique solution of* (1.8) *with boundary condition $a = 1$ on $\partial\Omega$ in some neighborhood $V$ containing $(x_0, y_0)$.*

*Proof.* It follows from Theorem 2.3.4 and the mapping $a = e^{\phi}$.

# 3. THE RBF METHOD

The radial basis function (RBF) interpolation method has become one of the primary tools for interpolating scattered data. The method's ability to handle arbitrarily scatted data and to provide good accuracy have made it particularly popular in several different types of application, such as medical imaging and neural networks. In this chapter we study basic properties about the RBF method and then apply them to our work. A RBF interpolation error estimate is reviewed in the last section of this chapter.

## 3.1 Introduction

The problem of interpolating scattered data occurs naturally in many areas of applied mathematics and the sciences. This includes surface reconstruction, image restoration and surface deformation.

The modern approach to scattered data interpolation can be traced back to the 1960s with the pioneering work of D. Shepard [43] on what is called today Shepard's interpolation. Shepards applied his method to surface modeling. In the 1970s, R. Hardy [24] developed different methods called the multiquadrics(MQ) and the inverse multiquadrics(IMQ).

From a mathematical point of view, a general scattered data interpolation problem can be formulated in the following way. Let $f$ be an unknown function from $\mathbb{R}^n$ to $\mathbb{R}$. Let $x_1, \ldots, x_k$ be a set of points in $\mathbb{R}^n$ and $s_1, \ldots, s_k$ be a set of values in $\mathbb{R}$. We wish to construct an interpolation $\tilde{f}$ to $f$ such that:

$$\tilde{f}(x_i) = s_i, i = 1, \ldots, k.$$

Note that in general there are infinitely many functions that would satisfy these

conditions. For instance the piecewise constant function, $\tilde{f}(x) = s_i$ if $x = x_i$ and 0 otherwise is always a solution. We usually assume that $f$ has some smoothness properties such as continuity or differentiability. Moreover, we often choose $\tilde{f}$ belonging to a certain class of functions. By constraining the solution space, we are implicitly making some assumptions on the type of function that $\tilde{f}$ is.

It is important to understand that interpolation is not always desirable. For example, our data may be corrupted by measurement errors, but we do want to construct an approximation which is close to the function values in some sense.

In one dimension, many methods can solve this problem, such as polynomial and Fourier interpolation. Most of these involve the same general idea: a set of basis function $F_j(x)_{j=1}^k$ is chosen such that a linear combination of these functions satisfies the interpolation conditions. Specifically, a function $s(x)$ is found of the form:

$$s(x) = \sum_{j=1}^{k} \lambda_j F_j(x). \tag{3.1}$$

The interpolation conditions lead to a linear system of equations which determines the coefficients $\lambda_j$. This system is guaranteed to be non-singular whenever the data points are distinct.

For data in more than one dimension, the methods described above no longer work. It can be shown that for any set of basis function $F_j(x)_{j=1}^k$ that are independent of the data points, there exists sets of distinct data points $x_1, \ldots, x_k$ such that the linear system of equations is singular. In other words, there is no interpolation of the form (3.1). This result is referred to as Haar's Theorem [20].

This non-singular problem can be solved by a different approach for creating a interpolation function. We use a linear combination of a single basis function that varies radially about its center instead of taking linear combination of a set of

basis functions that are independent of the data points. This approach, provided by R.Hardy [24], is referred to as the radial basis function (RBF) method.

The RBF method is a generalized version of the MQ method constructed in 1968 by R.Hardy [24]. He developed this method to solve a problem from cartography. Following the publication of Hardy's MQ method, many people began using the method in other areas, such as problems in hydrology(approximating the average rainfall in a region), photogrammetry (reconstructing images), and geology (approximating ground water levels from well-logs). See [25] for more details.

Around the same time, methods similar to the MQ method began appearing. J.Duchon [12] [13] took a variational approach and developed interpolants that led to thin plate splines.

A mathematical formulation of the RBF method was finally provided in 1986 by Micchelli [31].

In [15], Richard Franke compared radial basis functions with some of the other methods, such as polynomial interpolation, tensor product methods and finite element methods. He conducted careful numerical experiments using different methods, including radial basis functions, and concluded that they provide excellent accuracy when interpolating scattered data. Franke summarized his result in [16], and found the RBF method to be the best method in this sense when compared to the other tested methods, thus providing an excellent reason for applying radial basis methods to our work.

## 3.2 Preliminaries

Radial basis function methods can provide interpolation to function values given at irregularly positioned points. Moreover, these interpolations are often excellent approximations to the underlying function, even when the number of interpolation

points is small.

They are conceptually easy to understand and the accuracy of approximation is usually very satisfactory. It is convenient to add a low-degree polynomial term to RBF interpolation in order to reproduce polynomial functions. The RBF kernels corresponding to the differential operators $\nabla^m$ have a non-trivial null space that contains exactly these polynomials.

In this section we review some definitions and conditions to the RBF method to guarantee its non-singularity.

Before we describe the RBF method, we give one more definition.

**Definition 3.2.1.** Let $\mathbb{P}_m^d$ be the space of all d-variate polynomials with a degree less than $m$. Furthermore, let $M$ denote the dimension of $\mathbb{P}_m^d$, then $M = \binom{m-1+d}{m-1}$.

**Definition 3.2.2.** (RBF interpolation method). Given a set of $k$ distinct data points $V = \{v_j\}_{j=1}^k$ and corresponding data values $\{f(v_j)\}_{j=1}^k$, a radial basis function approximation with a polynomial term can be written as

$$s(v) = \sum_{j=1}^{k} \lambda_j F(\parallel v - v_j \parallel) + \sum_{i=1}^{M} c_i p_i(v), v \in \mathbb{R}^d \tag{3.2}$$

where $\{p_i(v)\}_{i=1}^M$ is a basis for $\mathbb{P}_m^d$ and $F(r)$, $r > 0$, is some real-valued radial function, also called the kernel of the RBF. The coefficients $\{\lambda_j\}_{j=1}^k$ and $\{c_i\}_{i=1}^M$ are chosen to satisfy the linear system:

$$\begin{aligned} s(v_i) &= f(v_i), \ j = 1, \ldots, k \\ \sum_{j=1}^{k} \lambda_j p_i(v_j) &= 0, \qquad i = 1, \ldots, M \end{aligned} \tag{3.3}$$

which are often called the natural boundary conditions.

Here, the set of scattered points $V$ is unisolvent for $\mathbb{P}_m^d$; that is, if $p \in \mathbb{P}_m^d$ and $p(v_j) = 0, j = 1, \ldots, k$ then $p = 0$. It guarantees that the interpolation method can reproduce the polynomial space $\mathbb{P}_m^d$. This can be a very useful property for many applications. For a choice of functions $F$ and polynomial orders $m$, the existence and uniqueness of the solution of the linear system (3.3) is ensured when $F$ is a conditionally positive definite function (see [31]).

**Definition 3.2.3.** Let $F : \mathbb{R}^d \to \mathbb{R}$ be a continuous function. We say that $F$ is conditionally positive definite of order $m \in \mathbb{N}_0$ , iff for all $N \in \mathbb{N}$, for all sets of pairwise distinct points $X = \{x_j\}_{j=1}^N \subseteq \mathbb{R}^d$, and all $\alpha \in \mathbb{R}^N \backslash \{0\}$ satisfying:

$$\sum_{j=1}^{N} \alpha_j p(x_j) = 0, \ \textit{for all } p \in \mathbb{P}_m^d \tag{3.4}$$

the quadratic form

$$\sum_{j,k=1}^{N} \alpha_j \alpha_k F(x_j - x_k) \tag{3.5}$$

is positive.

**Theorem 3.2.1** (Uniqueness, [31])**.** *Let $F$ be conditionally positive definite of order $m$. The function $s$ defined in equation* (3.2) *is the unique solution to the problem of interpolation with polynomial reproduction, provided that $c$ and $\lambda$ are required to satisfy* (3.3)*.*

Typical examples for kernels $F(r)$ which satisfy the above requirement include:

- Gaussian $F(r) = e^{-\epsilon r^2}$
- Linear $F(r) = r$

- Thin-plate Splines $F(r) = r^2 \ln r$ (in two dimensions)
- Hardy's MultiQuadrics (MQ): $F(r) = (r^2 + c^2)^{1/2}$
- Inverse MultiQuadrics (IMQ): $F(r) = (r^2 + c^2)^{-1/2}$
- Wendland's compactly supported ([46]): $F(r) = (1 - r)_+^4(4r + 1)$

Schoenberg [42] provided a sufficient condition to guarantee conditionally positive definiteness of $F$. To understand his result it is necessary to introduce the idea of completely monotone function.

**Definition 3.2.4.** (Completely Monotone Function). A function $f$ is called completely monotone on $[0, \infty)$ if

1. $f \in C[0, \infty)$.
2. $f \in C^\infty(0, \infty)$.
3. $(-1)^k f^{(k)}(r) \geq 0$ for $r > 0$ and $k = 0, 1, 2, ....$

We denote the class of such functions by $CM[0, \infty)$.

For example, The function $f(r) = \dfrac{1}{r}$ is in $CM[0, \infty)$. In general, the following theorem characterizes the completely monotone function.

**Theorem 3.2.2** (Bernstein-Widder [47])**.** *A function $f$ belongs to $CM(0, \infty)$ if and only if there is a nonnegative Borel measure $d\eta$ defined on $[0, \infty)$ such that*

$$f(\sigma) = \int_0^\infty e^{-\sigma t} d\eta(t) \tag{3.6}$$

*is convergent for $0 < \sigma < \infty$. Moreover, $f$ is in $CM[0, \infty)$ if and only if the integral converges for $\sigma = 0$.*

Schoenberg [42] found the connection between positive definite functions and completely monotone functions. His result is as follows:

**Theorem 3.2.3** (Schoenberg [42]). *A radical function $F(r)$ is positive definite on $R^n$ for all $n$ if and only if $f(r) := F(\sqrt{r})$ is in $CM[0,\infty)$. In other words, $f(r)$ is completely monotone function and continuous at $r = 0$.*

From this theorem we can conclude, for example, the Gaussian kernel is positive definite since for $k = 0, 1, 2...$ and $r > 0$,

$$f(r) = F(\sqrt{r}) = e^{-\epsilon r} \Rightarrow (-1)^k f^{(k)}(r) = \epsilon^k e^{-\epsilon r} > 0.$$

But we can not make the same conclusion for the MQ and linear kernels since in both cases $f(r) > 0$ and $f'(r) > 0$. However, Micchelli [31] generalizes Schoenberg's theorem to the $m = 1$ case.

**Theorem 3.2.4** (Micchelli [31]). *A continuous radical function $F(r)$ is an order 1 conditionally positive definite function on $R^n$ for all $n$ if and only if $-\frac{d}{dr}F(\sqrt{r})$ is completely monotonic on $(0,\infty)$.*

There is also an analogue for $m > 1$ proved by K.Guo, S.Hu and X.Sun [19].

**Theorem 3.2.5.** *A continuous radical function $F(r)$ is an order $m$ conditionally positive definite function on $R^n$ for all $n$ if and only if $(-1)^m \frac{d^m}{dr^m}F(\sqrt{r})$ is completely monotonic on $(0,\infty)$.*

Consider Duchon's thin plate spline kernel in two dimensions, $F(r) = r^2 \ln r$. To apply our theorem, we note that $F(\sqrt{r}) = \frac{1}{2} r \ln r$. It is easy to verify that $(-1)^2 \frac{d^2}{dr^2} r \ln r = \frac{1}{r}$, which is completely monotonic on $(0,\infty)$ as we mentioned before. Therefore, Duchon's thin plate spline kernel in two dimensions is a conditionally positive definite function of order 2.

The thin plate spline kernel is of particular practical interest since it is related to the minimization of a bending energy. In fact Duchon [12] derived (3.3) as the solution to a variational problem when $d = 2$. He proved that the function $s$ given by (3.2) minimizes the following integral:

$$\int [s_{x_1x_1}]^2 + [s_{x_2x_2}]^2 + [s_{x_3x_3}]^2. \tag{3.7}$$

One can also find an alternative way to prove this in Powell [39], [40].

In $n$ dimensions, the idea of thin plate splines is to choose a function $f(x)$ that exactly interpolates the data and also minimizes the bending energy,

$$\int |D^2 f|^2 dX \tag{3.8}$$

where $D^2 f$ is the matrix of second-order partial derivatives of $f$ and $|D^2 f|^2$ is the sum of squares of the matrix entries.

If $k > n/2$ is an integer, then we can define the thin plate spline corresponding to $n$ and $k$ as follows:

$$F_{n,k}(x) = c_{n,k}\|x\|_2^{2k-n}, \quad n \; odd$$
$$F_{n,k}(x) = c_{n,k}\|x\|_2^{2k-n} ln\|x\|_2, \quad n \; even$$

where $c_{n,k}$ is a constant chosen so that the distributional Fourier transform $F_{n,k}(\omega) = \|\omega\|_2^{-2k}$, if $\omega \neq 0$. This function $F_{n,k}$ is conditionally positive definite of order $k - \lceil n \rceil + 1$ (Note: $\lceil n \rceil$ is the ceiling function, which denotes the smallest following integer of $n$.)

Franke [16] considered different radial basis functions including the thin plate spline in his comparison of multivariate approximation methods. He found that this

thin plate spline provided the most accurate interpolation of all methods tested for interpolation in two dimensions (more generally, in even dimensions).

We use thin-plate splines of order $m = 2$ to be our basis function in the numerical simulations. Compactly supported radial basis functions have been invented for the purpose of getting finite-element type approximations (Brenner and Scott [6]). In future work, we will consider local error estimates with compactly supported RBFs [17], [18], [22], [23].

By definition 3.2.2, we are looking for approximation for our solution $u(x, y)$ of form:

$$\tilde{u}(x, y) = \sum_{j=1}^{k} \lambda_j F_j(x, y) + P(x, y) \tag{3.9}$$

where $F_j(x, y)$ is the RBF and $P(x, y)$ is a low-degree polynomial:

$$P(x, y) = c_1 + c_2 x + c_3 y. \tag{3.10}$$

The unknown coefficients $\lambda_j$ and $c_i$ are determined from the interpolation conditions and the following constraints:

$$\sum_{i=1}^{k} \lambda_i = \sum_{i=1}^{k} \lambda_i x_i = \sum_{i=1}^{k} \lambda_i y_i = 0. \tag{3.11}$$

Once coefficients $\lambda_j$ and $c_i$ are found, (3.9) can be used to estimate value of the function $u(x, y)$ and its derivatives at any point.

## 3.3 RBF interpolation

Most of the error estimates for RBF interpolation depended on using reproducing kernel Hilbert space or native space methods. But these error estimates have their own limitations. In many applications of RBF methods, the functions generating the

data may not have the right properties to be in native space that depends on the kernel $F(r)$.

We assume for the rest of this section that our RBF kernel $F(r)$ has either a classical Fourier transform that satisfies

$$c_1(1+\|\omega\|_2^2)^{-\tau} \leq \hat{F}(\omega) \leq c_2(1+\|\omega\|_2^2)^{-\tau}, \quad \omega \in \mathbb{R}^n$$

or a generalized Fourier transform that satisfies

$$c_1\|\omega\|_2^{-2\tau} \leq \hat{F}(\omega) \leq c_2\|\omega\|_2^{-2\tau}, \quad \omega \in \mathbb{R}^n \backslash 0,$$

where we take $\tau > n/2$. It's easy to verify that the thin-plate splines satisfy the conditions.

The next theorem is related to RBF interpolation, which is vital in proving the error estimates of our reconstruction.

Above all, we introduce some quantities that will be useful in the theorem.

**Definition 3.3.1.** Let $X = \{v_1, v_2, ...v_N\}$ be a finite set of points in $\Omega$. The mesh norm for $X$ relative to $\Omega$ is given by:

$$h_{X,\Omega} = \sup_{v \in \Omega} \inf_{v_j \in X} \|v - v_j\|_2. \tag{3.12}$$

It measures the maximum distance any point in $\Omega$ can be from $X$ and expresses how well the data fills a region of interest $\Omega$. The mesh norm can be used to bound the approximation error.

**Definition 3.3.2.** The separation distance is given by

$$q_X = \inf_{j \neq k} \|v_j - v_k\|_2. \tag{3.13}$$

This quantity measures how close the data are together.

Finally, we have the mesh ratio $\rho = h/q \geq 1$ provides a measure of how uniformly points in $X$ are distributed in $\Omega$.

Now one result concerning the RBF interpolation error estimate is presented here:

**Theorem 3.3.1** (RBF Interpolation Inequality, [35])**.** *Let $\tau = k + s$ with $0 \leq s < 1$ and $k \in \mathbb{N}$ with $k > n/2$. If $f \in W^{\tau,2}(\Omega)$, then*

$$\|f - \tilde{f}\|_{W^{\beta,2}(\Omega)} \leq C h_{X,\Omega}^{\tau-\beta} \|f\|_{W^{\tau,2}(\Omega)}, \qquad 0 \leq \beta \leq \tau \tag{3.14}$$

*where $\tau$ depends on the choice of the kernel $F(r)$ and $\tilde{f}$ is the RBF interpolation of $f$.*

The key to prove this theorem is the following two lemmas:

**Lemma 3.3.2** ( [34], Prop.3.2 and Cor.3.6)**.** *Under the assumptions made in Theorem 3.3.1, we have the estimate:*

$$\|f - \tilde{f}\|_{L^2(\Omega)} \leq C h_{X,\Omega}^{\tau} \|f\|_{W^{\tau,2}(\Omega)}. \tag{3.15}$$

**Lemma 3.3.3** ( [35], Prop.12.1.5 and Theorem 12.2.7)**.** *Suppose $T : W^{\tau,2}(\Omega) \to W^{\tau,2}(\Omega)$ is a linear operator, where $\Omega \in \mathbb{R}^n$ is a Lipschitz domain. We also assume*

*that the operator is bounded in the following way:*

$$\|Tf\|_{L^2(\Omega)} \leq C_1 \|f\|_{W^{\tau,2}(\Omega)}, \quad f \in W^{\tau,2}(\Omega) \tag{3.16}$$

$$\|Tf\|_{W^{\tau,2}(\Omega)} \leq C_2 \|f\|_{W^{\tau,2}(\Omega)}, \quad f \in W^{\tau,2}(\Omega). \tag{3.17}$$

*Then, for every* $0 < \beta < \tau$*, we also have*

$$\|Tf\|_{W^{\beta,2}(\Omega)} \leq C_1^{1-\beta/\tau} C_2^{\beta/\tau} \|f\|_{W^{\tau,2}(\Omega)}. \tag{3.18}$$

We refer to [33], [34] and [35] for details.

# 4. ERROR ESTIMATE

In this chapter, we will establish an error estimate for our approximation $\tilde{a}$ to the unknown coefficient $a$ under certain assumptions.

The key ingredients to the error estimate result are a PDE estimate, a Sobolev embedding estimate and an RBF interpolation estimate.

For the remaining of this chapter, let $\tilde{u}$ denote the RBF interpolation of $u$ from the observed data and $\tilde{a}$ denote the approximate value of $a$ satisfying (1.8).

## 4.1 PDE estimate

To obtain our error estimate, we make the following assumptions:

**Assumption 4.1.1.**

- *For simplicity, we assume* $f = 0$.
- *The solution* $u$ *of the equation* $\nabla \cdot (a\nabla u) = 0$ *exists.*
- *There exists a constant* $c > 0$, *such that* $c^{-1} \leq a(x, y) \leq c$, *i.e., uniformly elliptic.*
- $u \in W^{\tau,2}(\Omega)$, *where* $\tau > 4$ *depends on the choice of kernel* $F(r)$.
- $|\nabla u| \geq \delta_1 > 0$, *i.e., there is no interior maximum in* $\Omega$.

*Remark:* Recall from Chapter 2, we don't have existence and uniqueness in general case so we must assume the existence of a sufficiently smooth solution $u$.

Besides these assumptions, we also require that the RBF interpolation $\tilde{u}$ satisfy $|\nabla \tilde{u}| \geq \delta_2 > 0$ to assure that $|\nabla \tilde{u}|$ is bounded away zero. First, we prove the following lemma, in which we claim that the length of each characteristic curve is finite. We denote $g$ as the diameter of the space $\Omega$.

**Lemma 4.1.1.** *Given that Assumptions 4.1.1 are satisfied, then any characteristic curve* $\Gamma$ *connecting two distinct points* $a_1, a_2 \in \Omega$ *from equations:*

$$\frac{d\psi}{ds} = -\frac{\nabla^2 u}{|\nabla u|}. \tag{4.1}$$

$$\frac{dx}{ds} = \frac{u_x}{|\nabla u|}. \tag{4.2}$$

$$\frac{dy}{ds} = \frac{u_y}{|\nabla u|}. \tag{4.3}$$

*If* $\Gamma(0) = a_1 \in \Omega$, $\Gamma(t) = a_2 \in \Omega$, *there exists a constant* $C(c, \delta_1, \|u\|_{L^\infty(\Omega)})$, *such that* $|t| \leq C$. *The length of the characteristic* $\Gamma$ *is equal to* $|t|$.

*Proof.* We introduce another function (a potential) via

$$\begin{aligned} a\frac{\partial u}{\partial x} &= \frac{\partial v}{\partial y}. \\ a\frac{\partial u}{\partial y} &= -\frac{\partial v}{\partial x}. \end{aligned}$$

The pair of functions $(u, v)$ form a new coordinate system with basic vectors:

$$e_1 = (\frac{u_x}{|\nabla u|}, \frac{u_y}{|\nabla u|}), e_2 = (\frac{v_x}{|\nabla v|}, \frac{v_y}{|\nabla v|}).$$

This coordinate system is also orthogonal since:

$$\begin{aligned} e_1 \cdot e_2 &= \frac{u_x v_x + u_y v_y}{|\nabla u||\nabla v|}. \\ &= \frac{u_x \cdot (-a u_y) + u_y \cdot (a u_x)}{|\nabla u||\nabla v|}. \\ &= 0 \end{aligned}$$

We denote $J$ as the Jacobian matrix and its determinant:

$$det(J) = |\frac{\partial(u,v)}{\partial(x,y)}| = u_x v_y + u_y v_x = a|\nabla u|^2. \tag{4.4}$$

By taking into account our assumption 4.1.1, $J$ is also nonsingular:

$$0 < \frac{1}{c} \cdot \delta_1^2 \leq det(J) \leq c \cdot |\nabla u|^2_{L^\infty} < \infty. \tag{4.5}$$

Thus we have a mapping between two coordinate systems:

$$\begin{pmatrix} du \\ dv \end{pmatrix} = J \begin{pmatrix} dx \\ dy \end{pmatrix}. \tag{4.6}$$

Or, in the opposite direction:

$$J^{-1} \begin{pmatrix} du \\ dv \end{pmatrix} = \begin{pmatrix} dx \\ dy \end{pmatrix}. \tag{4.7}$$

Let's compute the length of characteristic curve in two different coordinate systems:

$$L = \int_0^t \sqrt{(\frac{dx}{ds})^2 + (\frac{dy}{ds})^2} ds \tag{4.8}$$

$$= \int_{a_1'}^{a_2'} \sqrt{(\frac{du}{ds}, \frac{dv}{ds})(J^{-1})' J^{-1} \begin{pmatrix} \frac{du}{ds} \\ \frac{dv}{ds} \end{pmatrix}} ds \tag{4.9}$$

where $a_1'$, $a_2'$ denote the transform of $a_1$,$a_2$ in $(u,v)$-coordinates.

Let us consider separately the left and right hand-side of the above equality. The

left hand-side equals $t$ plainly follows from (4.1). Indeed,

$$\int_0^t \sqrt{(\frac{dx}{ds})^2 + (\frac{dy}{ds})^2} ds = \int_0^t 1 \cdot ds = t. \tag{4.10}$$

On the right hand-side, by taking into account (4.5) and also:

$$\frac{dv}{ds} = v_x \frac{dx}{ds} + v_y \frac{dy}{ds} = 0. \tag{4.11}$$

We get:

$$\begin{aligned}
\int_{a_1'}^{a_2'} \sqrt{(\frac{du}{ds}, \frac{dv}{ds})(J^{-1})' J^{-1} \begin{pmatrix} \frac{du}{ds} \\ \frac{dv}{ds} \end{pmatrix}} ds &\leq \frac{c}{\delta_1^2} \int_{a_1'}^{a_2'} \sqrt{(\frac{du}{ds}, \frac{dv}{ds}) \begin{pmatrix} \frac{du}{ds} \\ \frac{dv}{ds} \end{pmatrix}} ds \quad (4.12) \\
&\leq \frac{c}{\delta_1^2} \cdot \|a_2' - a_1'\| \quad (4.13) \\
&\leq \frac{c}{\delta_1^2} \cdot 2 \cdot \|u\|_{L^\infty(\Omega)}. \quad (4.14)
\end{aligned}$$

Finally, combining (4.10) with (4.14), we obtain our estimate:

$$|t| \leq C(c, \delta_1, \|u\|_{L^\infty(\Omega)}). \tag{4.15}$$

We use this lemma to prove the following PDE error estimate between exact value $a$ and approximate value $\tilde{a}$.

**Theorem 4.1.2.** *Given that Assumptions 4.1.1 are satisfied, then there exists a positive constant $C = C(g, \|\nabla u\|_{L^\infty}, \|\nabla^2 u\|_{L^\infty}, \delta_1, \delta_2)$, such that, for any $0 < \mu \leq 1$, the following inequality holds:*

$$\|a - \tilde{a}\|_{L^\infty} \leq C(\|\nabla^2(u - \tilde{u})\|_{0,\mu;\Omega} + \|\nabla(u - \tilde{u})\|_{0,\mu;\Omega}). \tag{4.16}$$

*Proof.* Based on the mapping $a(x,y) = e^{\phi(x,y)}$, we have:

$$\begin{aligned} |a - \tilde{a}| &= |e^{\phi} - e^{\tilde{\phi}}| && (4.17)\\ &\leq C_1 |\phi - \tilde{\phi}|. && (4.18) \end{aligned}$$

Note that $\phi$ is the solution of the following system of ODE:

$$\begin{aligned} \frac{d\phi}{ds} &= -\frac{\nabla^2 u}{|\nabla u|}. \\ \frac{dx}{ds} &= \frac{u_x}{|\nabla u|}. \\ \frac{dy}{ds} &= \frac{u_y}{|\nabla u|}. \end{aligned} \tag{4.19}$$

Now for each characteristic curve, we can write:

$$\begin{aligned} |\phi - \tilde{\phi}| &= |\int_0^t (\frac{d\phi}{ds} - \frac{d\tilde{\phi}}{ds}) ds| && (4.20)\\ &= \int_0^t |\frac{\nabla^2 u}{|\nabla u|} - \frac{\nabla^2 \tilde{u}}{|\nabla \tilde{u}|}| ds && (4.21)\\ &= \int_0^t |\frac{\nabla^2 u |\nabla \tilde{u}| - \nabla^2 \tilde{u} |\nabla u|}{|\nabla u||\nabla \tilde{u}|}| ds && (4.22)\\ &= \int_0^t |\frac{(\nabla^2 u - \nabla^2 \tilde{u})|\nabla \tilde{u}| + \nabla^2 \tilde{u}(|\nabla \tilde{u}| - |\nabla u|)}{|\nabla u||\nabla \tilde{u}|}| ds. && (4.23) \end{aligned}$$

Apply Lemma 4.1.1 to (4.23), we obtain:

$$|\phi - \tilde{\phi}| \leq C_2 (\frac{\|\nabla^2 (u - \tilde{u})\|_{L^\infty}}{|\nabla u|} + \frac{\|\nabla^2 \tilde{u}\|_{L^\infty} \|\nabla (u - \tilde{u})\|_{L^\infty}}{|\nabla u||\nabla \tilde{u}|}). \tag{4.24}$$

Then by Assumptions 4.1.1

$$\begin{aligned} |\phi - \tilde{\phi}| &\leq C_2\left(\frac{\|\nabla^2(u-\tilde{u})\|_{L^\infty}}{\delta_1} + \frac{\|\nabla^2\tilde{u}\|_{L^\infty}\|\nabla(u-\tilde{u})\|_{L^\infty}}{\delta_1\delta_2}\right) \\ &\leq C_2\left(\frac{\|\nabla^2(u-\tilde{u})\|_{0,\mu;\Omega}}{\delta_1} + \frac{\|\nabla^2\tilde{u}\|_{L^\infty}\|\nabla(u-\tilde{u})\|_{0,\mu;\Omega}}{\delta_1\delta_2}\right). \end{aligned}$$

Together with (4.18), let $C$ be a positive constant:

$$C = C(C_1, C_2, g, \|\nabla u\|_{L^\infty}, \|\nabla^2 u\|_{L^\infty}, \delta_1, \delta_2),$$

we obtain:

$$|a - \tilde{a}| \leq C(\|\nabla^2(u-\tilde{u})\|_{0,\mu;\Omega} + \|\nabla(u-\tilde{u})\|_{0,\mu;\Omega}). \tag{4.25}$$

This is true for every characteristic curve, hence, we have:

$$\|a - \tilde{a}\|_{L^\infty} \leq C(\|\nabla^2(u-\tilde{u})\|_{0,\mu;\Omega} + \|\nabla(u-\tilde{u})\|_{0,\mu;\Omega}). \tag{4.26}$$

## 4.2 Sobolev embedding estimate

Recall one case of General Sobolev inequalities from Chapter 2:

**Theorem 4.2.1** (General Sobolev inequalities)**.** *Let $\Omega$ be a bounded open subset of $R^n$, with a $C^1$ boundary. Assume $u \in W^{k,p}(\Omega)$. If $k > \frac{n}{p}$, then $u \in C^{k-[\frac{n}{p}]-1,\mu}(\Omega)$, where $\mu = [\frac{n}{p}] + 1 - \frac{n}{p}$ if $\frac{n}{p}$ is not an integer, or $\mu$ is any positive number $< 1$, if $\frac{n}{p}$ is an integer. We have in addition the estimate:*

$$\|u\|_{C^{k-[\frac{n}{p}]-1,\mu}(\Omega)} \leq C\|u\|_{W^{k,p}(\Omega)} \tag{4.27}$$

*the constant $C$ depending only on $k, p, n, \mu$ and $\Omega$.*

The aim of this section is to present a Sobolev embedding error estimate based

on Theorem 4.2.1.

In order to do this, we provide the following lemma which would be helpful.

**Lemma 4.2.2.** *Let $\Omega$ be a bounded open subset of $R^2$, with a $C^1$ boundary. Assume $u \in W^{2,2}(\Omega)$. For any $0 < \mu < 1$, we have the following inequality:*

$$\|u\|_{0,\mu;\Omega} \leq C\|u\|_{W^{2,2}(\Omega)}. \tag{4.28}$$

*Proof.* Let $n = p = 2$, $0 < \mu < 1$ and $k = 2$. This lemma is a direct result of Theorem 4.2.1.

**Theorem 4.2.3.** *Given that Assumptions 4.1.1 are satisfied, then there exists a positive constant $C$, such that, for any $0 < \mu < 1$, the following inequality holds:*

$$\|a - \tilde{a}\|_{L^\infty} \leq C(\|u - \tilde{u}\|_{W^{4,2}(\Omega)}). \tag{4.29}$$

*Proof.* Using the estimate (4.16) and Lemma 4.2.2, we obtain:

$$\begin{aligned}
\|a - \tilde{a}\|_{L^\infty} &\leq C(\|\nabla^2(u - \tilde{u})\|_{0,\mu;\Omega} + \|\nabla(u - \tilde{u})\|_{0,\mu;\Omega}). \\
&\leq C(\|\nabla^2(u - \tilde{u})\|_{W^{2,2}(\Omega)} + \|\nabla(u - \tilde{u})\|_{W^{2,2}(\Omega)}). \\
&\leq C(\|u - \tilde{u}\|_{W^{4,2}(\Omega)} + \|u - \tilde{u}\|_{W^{3,2}(\Omega)}). \\
&\leq C(\|u - \tilde{u}\|_{W^{4,2}(\Omega)}).
\end{aligned}$$

## 4.3 RBF interpolation estimate

In this section we derive an inquality between the exact value $a$ and the approximate value $\tilde{a}$ based on the RBF interpolation inequality from Chapter 3.

The main result is stated in the following theorem.

**Theorem 4.3.1.** *Given that Assumptions 4.1.1 are satisfied, then there exists a positive constant $C$, such that the following inequality holds:*

$$\|a - \tilde{a}\|_{L^\infty} \leq Ch^{\tau-4}(\|u\|_{W^{\tau,2}(\Omega)}),\ \tau > 4, \tag{4.30}$$

*where $\tau$ depends on the choice of the kernel $F(r)$.*

*Proof.* We note that $\tilde{u}$ is the RBF interpolation of $u$.

Let $\beta = 4$ and $n = 2$, by Theorem 3.3.1, the following estimate holds:

$$\|u - \tilde{u}\|_{W^{4,2}(\Omega)} \leq Ch^{\tau-4}(\|u\|_{W^{\tau,2}(\Omega)}). \tag{4.31}$$

Then using the estimate (4.29),

$$\begin{aligned} \|a - \tilde{a}\|_{L^\infty} &\leq C(\|u - \tilde{u}\|_{W^{4,2}(\Omega)} && (4.32)\\ &\leq Ch^{\tau-4}(\|u\|_{W^{\tau,2}(\Omega)}), && (4.33) \end{aligned}$$

and the theorem is proved.

*Remark:* The requirement $\tau > 4$ is sharp, and the space $W^{\tau,2}(\Omega)$ is "optimal", in the sense that if $u$ belongs to a weaker space ($W^{\tau,2}(\Omega)$, $\tau \leq 4$), $\nabla^2 u$ is not necessarily Lipschitz continuous, and the characteristic system (2.36) may not have a unique solution.

# 5. NUMERICAL METHODS AND RESULTS

In this chapter, we describe an algorithm for the approximation of $a$. Then, we will test the algorithm on some examples. We also would like to apply our algorithm to check the error estimate inequality from last chapter. To test our algorithm, we assume that we know $a$, $f$,$u$ perfectly. Here $u$ is a solution of the equation $-\nabla \cdot (a\nabla u) = f$. We also choose k interior points by $u(x_i, y_i) = g_i$, $i = 1, 2, ..., k$. We provide two different algorithms based on the boundary condition of $a$. To make sure our algorithms work, we also need to assume $|\nabla \tilde{u}| \neq 0$.

## 5.1 Case I: $a = 1$ on the boundary $\partial\Omega$

Our model problem is to reconstruct coefficient $a \in C^\infty(\bar{\Omega})$ from the elliptic equation $-\nabla \cdot (a\nabla u) = f$ with finite data. As described above, after mapping $a(x, y) = e^{\phi(x,y)}$, this ultimately leads to a system of ordinary differential equations (2.36) along the characteristic curves. Let $\tilde{u}$ be the RBF interpolation of $u$ and compute $\nabla\tilde{u}$ and $\nabla^2\tilde{u}$ by RBF method. Then, we can recover $\tilde{\phi}$ along each characteristic curve from the following system of ODEs:

$$\begin{aligned} \frac{d\phi}{ds} &= -\frac{\nabla^2\tilde{u}}{|\nabla\tilde{u}|} + \frac{e^{-\phi}\cdot f}{|\nabla\tilde{u}|}. \\ \frac{dx}{ds} &= \frac{\tilde{u}_x}{|\nabla\tilde{u}|}. \\ \frac{dy}{ds} &= \frac{\tilde{u}_y}{|\nabla\tilde{u}|}. \end{aligned} \tag{5.1}$$

with initial data $\phi(x_0, y_0) = 0$ on the boundary $\partial\Omega$.

Finally, we have our approximation to $a$ by inverting the mapping and denote it as $\tilde{a}$.

*Test Case I*: Let $\Omega$ be $[-1, 1]^2$, we consider the following test case with radial

parameter $a$.

Let

$$a(r) = \begin{cases} 2 - 2|r|^2, & |r| < \sqrt{2}/2, \\ 1, & \text{otherwise.} \end{cases} \tag{5.2}$$

$f(x, y) = 0$. And $u(x, y)$ is the numerical solution of the equation $-\nabla \cdot (a\nabla u) = f$.

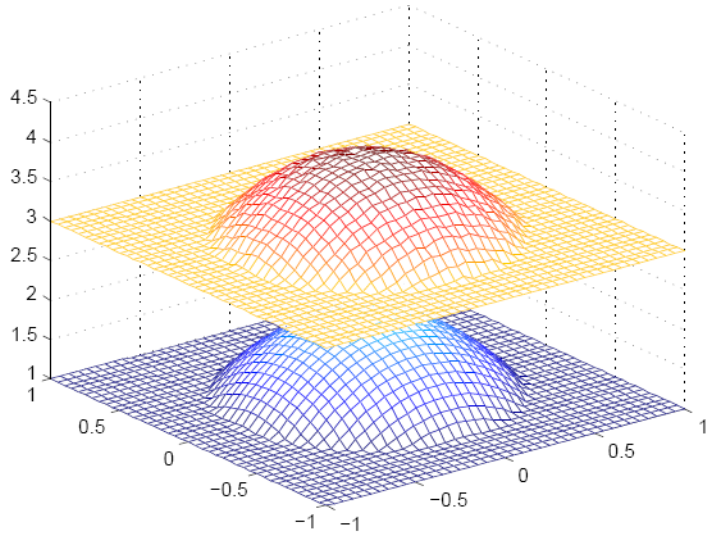


Figure 5.1: The upper graph shows the approximation $\tilde{a}$ of the model problem and the lower graph shows the exact parameter of the model problem.

Given $k = 400 = 20 \cdot 20$ uniformly distributed interior points in $\Omega$, a plot of the comparison between the approximation $\tilde{a}$ and the exact $a$ can be seen in Figure 5.1.

Figure 5.3 is a logarithmic plot of the error estimates for the specific number of uniformly distributed interior points. It shows that the the numerical error is exponentially decreasing.

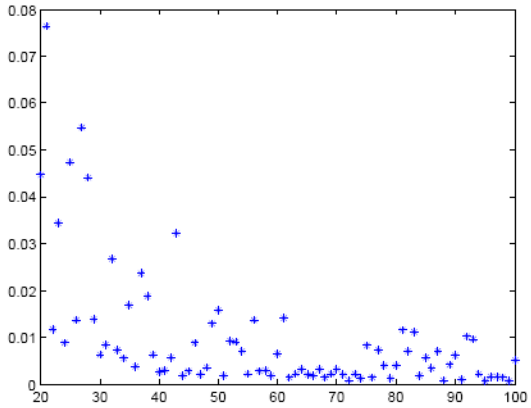


Figure 5.2: Relationship between the number of interior points $k$ and the error estimate $\|\tilde{a} - a\|_{L^\infty}$.

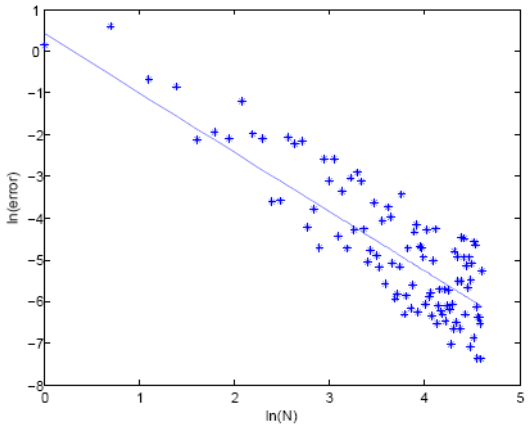


Figure 5.3: Relationship between the number of interior points $k$ and the error estimate $\|\tilde{a} - a\|_{L^\infty}$ in log-log plane in case I. The slope of regression line is $-1.42$ and the power of mesh norm $h$ is 2.84.

Here is another special test case with sequence $a_n$. We apply our algorithm when the parameter $a$ is close to a discontinuous function.

*Test Case II*: Let

$$a_n(r) = \begin{cases} 1/3, & |r| \leq 1/2 - 1/n, \\ \dfrac{2nr - n + 4}{6}, & 1/2 - 1/n < |r| < 1/2 + 1/n, \\ 1, & |r| \geq 1/2 + 1/n, \end{cases} \tag{5.3}$$

where $n > 2$.

The sequence $a_n$ converges pointwise to the function, $a$ defined by

$$a(r) = \begin{cases} 1/3, & |r| < 1/2, \\ 2/3, & |r| = 1/2, \\ 1, & |r| > 1/2. \end{cases} \tag{5.4}$$

Although all the functions $a_n$ are continuous, the limit function $a$ is not.

In Figure 5.4 the reconstruction is displayed together with the exact parameter $a_{50}$, given $k = 100$ uniformly distributed interior points.

And Figure 5.5 and 5.6 describe the error estimate between $a_{50}$ and $\tilde{a}_{50}$. Here we choose $k = N \cdot N$ uniformly distributed interior points.

Next, we take a different approach to our test case I. Because the difficulty of finding $k$ uniformly distributed interior points is not practical, we try to choose $k$ random interior points to make sure the algorithm still works.

To be clear, we test 20 times for each number $k$, which is the whole number of interior points, then we use average mesh norm $\bar{h}$ and average error estimate $\|\tilde{a} - a\|_{L^\infty}$ to compare. First, we would like to show the relationship between $\bar{h}$ and $k$ as follows:

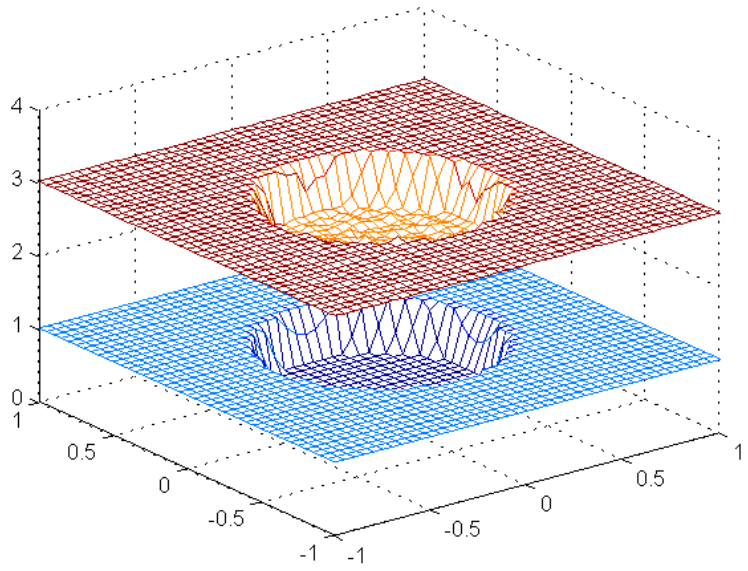


Figure 5.4: The upper graph shows the approximation $\tilde{a}_{50}$ of the model problem and the lower graph shows the exact parameter $a_{50}$ of the model problem, given $k = 100 = 10 \cdot 10$ equally spaced lattice points.

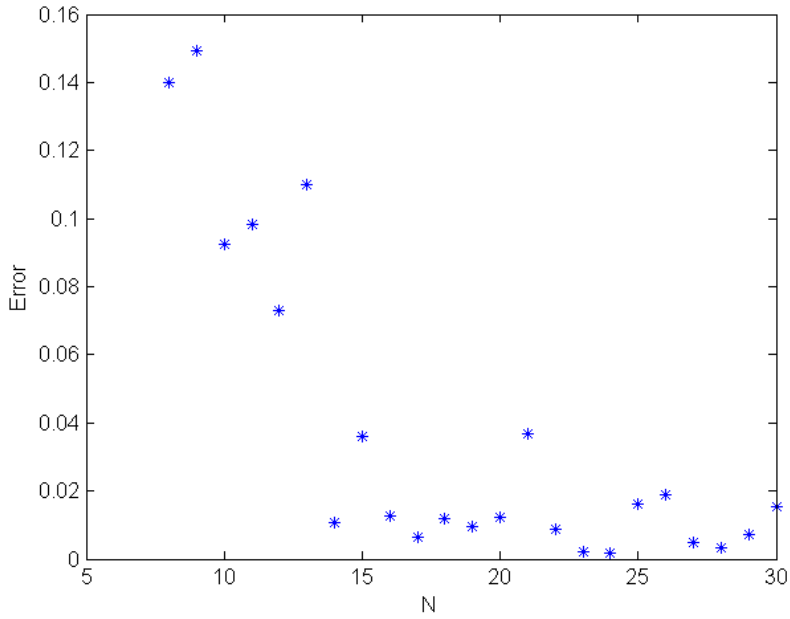


Figure 5.5: Relationship between the number of interior points $k$ and the error estimate $\|\tilde{a}_{50} - a_{50}\|_{L^\infty}$.

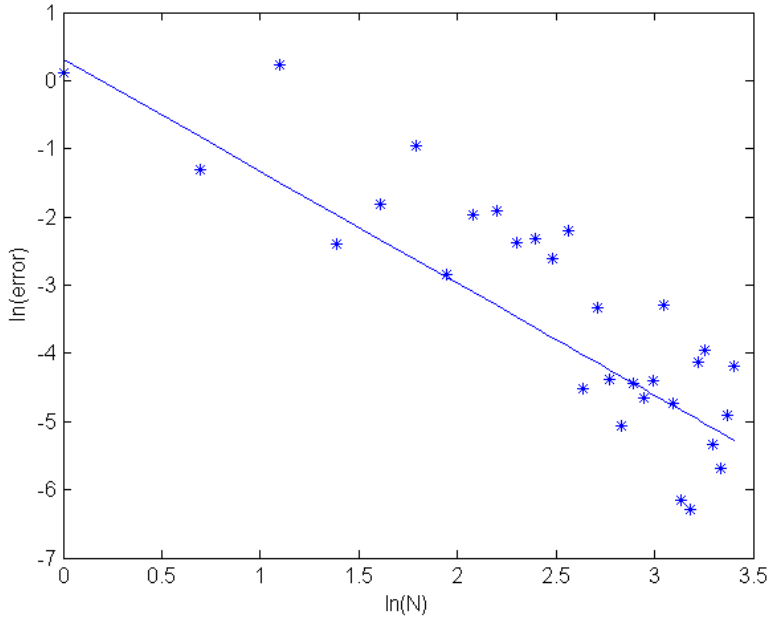


Figure 5.6: Relationship between the number of interior points $k$ and the error estimate $\|\tilde{a}_{50} - a_{50}\|_{L^\infty}$ in log-log plane. The slope of regression line is $-1.643$ and the power of mesh norm $h$ is 1.643.

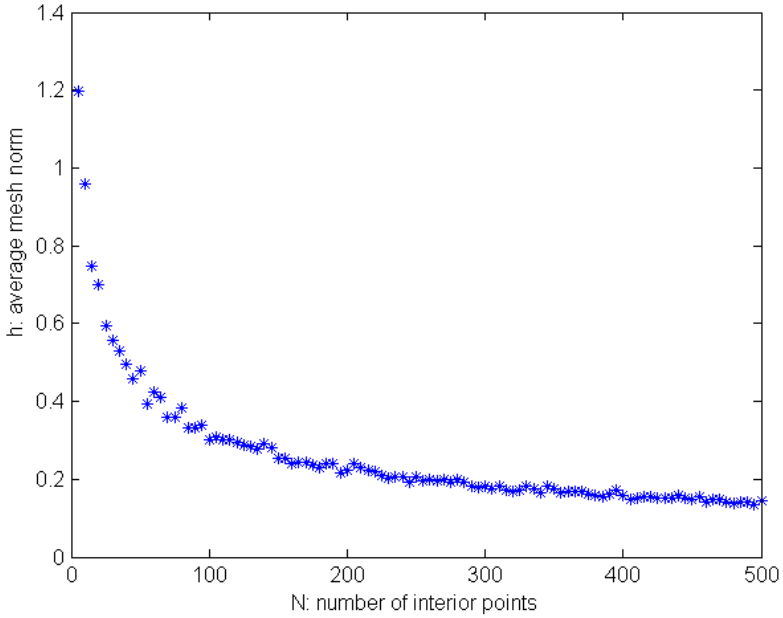


Figure 5.7: Relationship between the number of interior points $k$ and the average mesh norm $\bar{h}$.

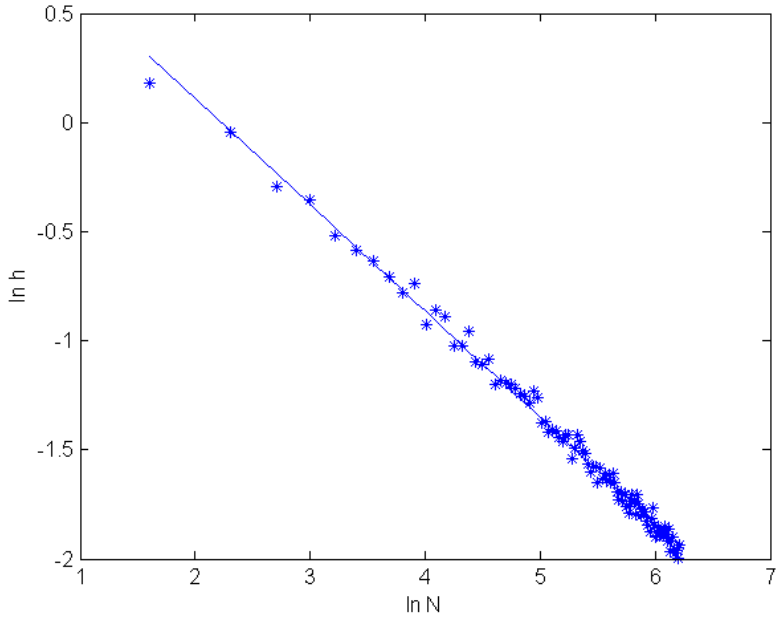


Figure 5.8: Relationship between the number of interior points $k$ and the average mesh norm $\bar{h}$ in log-log plane. The slope of regression line is $-0.4876$.

From the graph in Figure 5.8, we notice that the average mesh norm $\bar{h}$ is not proportional to $\sqrt{k}$ as in the uniformly distributed case, but still very close.

Next, we show the relationship between average mesh norm $\bar{h}$ and our average logarithmic error estimate $\|\tilde{a} - a\|_{L^\infty}$ in Figure 5.9.

The graph illustrates that the power of mesh norm compared to error estimate in this case is lower than in the uniformly distributed case.

Finally, we would like to present series of plots between the exact value of $a$ and our approximation $\tilde{a}$ while increasing the total number of random interior points. In each plot, the upper graph shows the approximation $\tilde{a}$ of the model problem and the lower graph shows the exact parameter of the model problem.

In the absence of a known boundary, one typical situation is the following case.

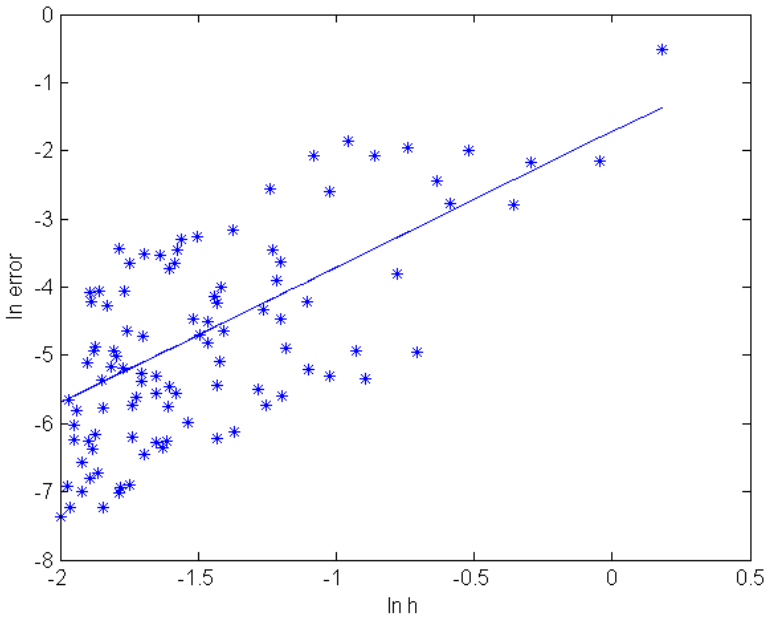


Figure 5.9: Relationship between the average mesh norm $\bar{h}$ and the error estimate $\|\tilde{a} - a\|_{L^\infty}$ in log-log plane. The slope of regression line is 1.986.

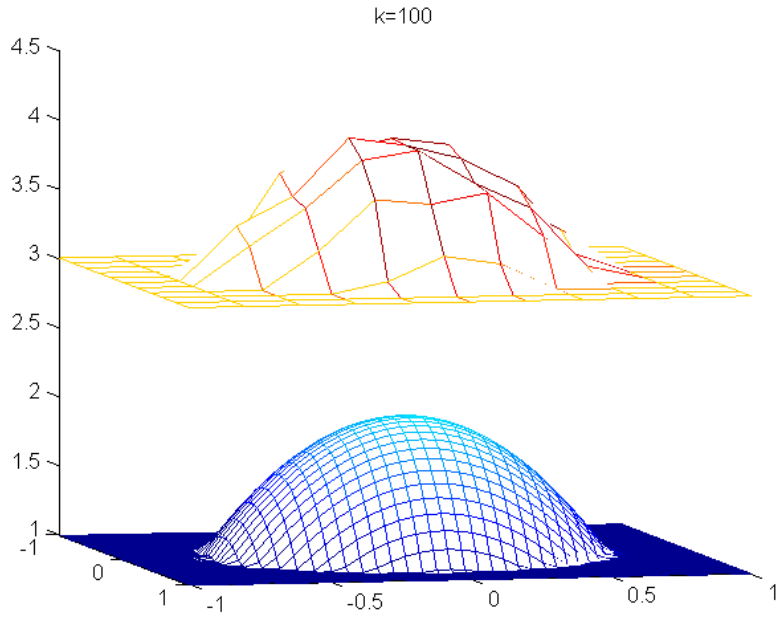


Figure 5.10: Comparison between the approximation $\tilde{a}$ and the exact value $a$ when $k = 100$ in case I.

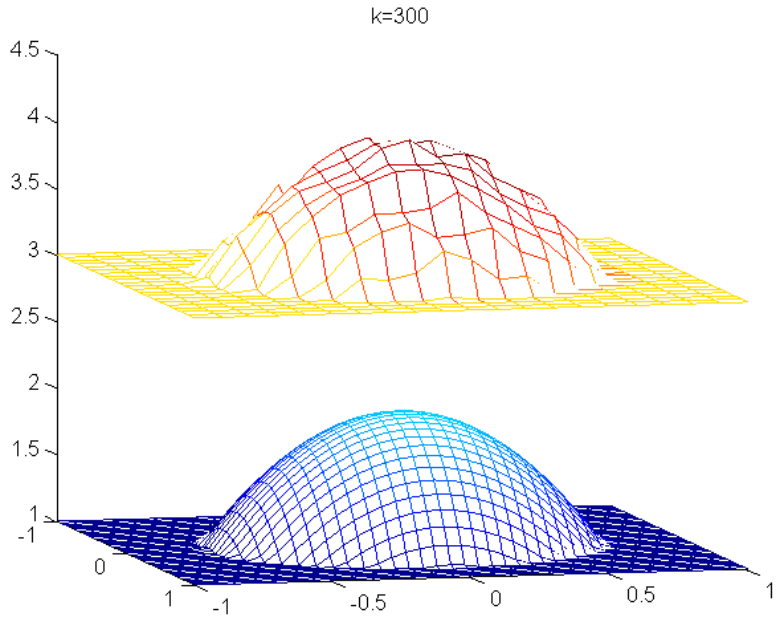


Figure 5.11: Comparison between the approximation $\tilde{a}$ and the exact value $a$ when $k = 300$ in case I.

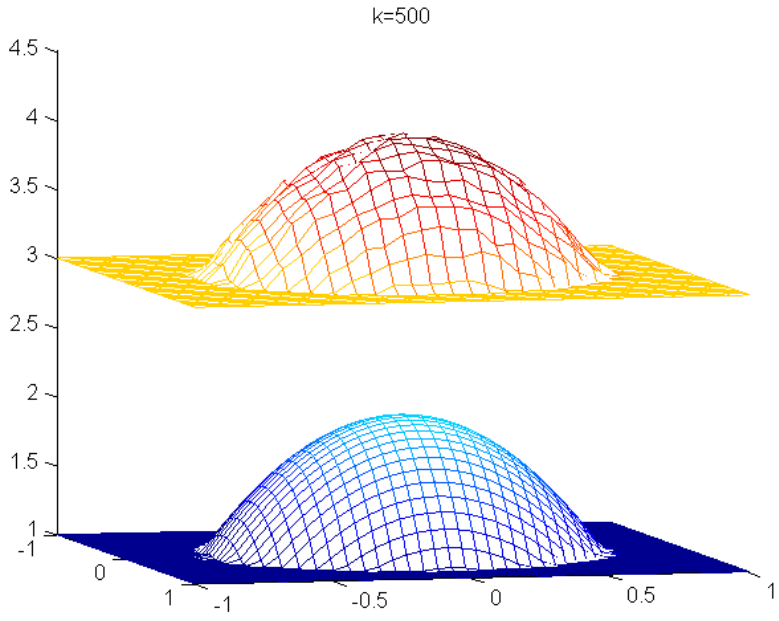


Figure 5.12: Comparison between the approximation $\tilde{a}$ and the exact value $a$ when $k = 500$ in case I.

## 5.2 Case II: $a = 1$ on the non-characteristic curve $\Lambda$

We assume that characteristic curves leaving $\Lambda$ cover the whole domain. In the algorithm we have proposed, we can still do the transformation and use RBF methods to compute $\tilde{u}$, $\nabla\tilde{u}$ and $\nabla^2\tilde{u}$. The problem is whether we can recover the coefficient $\phi$ from the ODEs by integration along the characteristic curves. Even we don't have any information on the boundary value, we can start our integration from the curve $\Lambda$ by letting $\phi(x_0, y_0) = 0$ and stop the integration when hitting the boundary. After doing this, the remain steps are the same as in case I.

Let's take a look at our test example. Let $\Omega$ be $[-1, 1]^2$, the exact value of $a$ defined as follows:

$$a(r) = 5 - 2|r|^2, \tag{5.5}$$

$f(x, y) = 0$. And $u(x, y)$ is the numerical solution of the equation $-\nabla \cdot (a\nabla u) = f$.

Let $\Lambda$ be the straight line $y = x - 2$ and also assume $a = 1$ on $\Lambda$.

Clearly, the characteristic curves leaving $\Lambda$ cover the whole domain.

In Figure 5.13$-$5.15 the approximations $\tilde{a}$ are displayed together with exact value $a$ at $k$ random interior points. In each plot, the upper graph shows the approximation $\tilde{a}$ of the model problem and the lower graph shows the exact parameter of the model problem.

One important thing gain from the figures is that the area close to the curve $\Lambda$ produces better approximation of exact $a$. The reason here is due to better RBF approximation of $\tilde{u}$, $\nabla\tilde{u}$ and $\nabla^2\tilde{u}$ near $\Lambda$.

Furthermore, in Figure 5.16, we have logarithmic plot showing the relationship between the average mesh norm $\bar{h}$ and average error estimates $\|\tilde{a} - a\|_{L^\infty}$:

As can be seen from Figure 5.16, the error estimate is not as good as in case I, but still reasonably accurate.

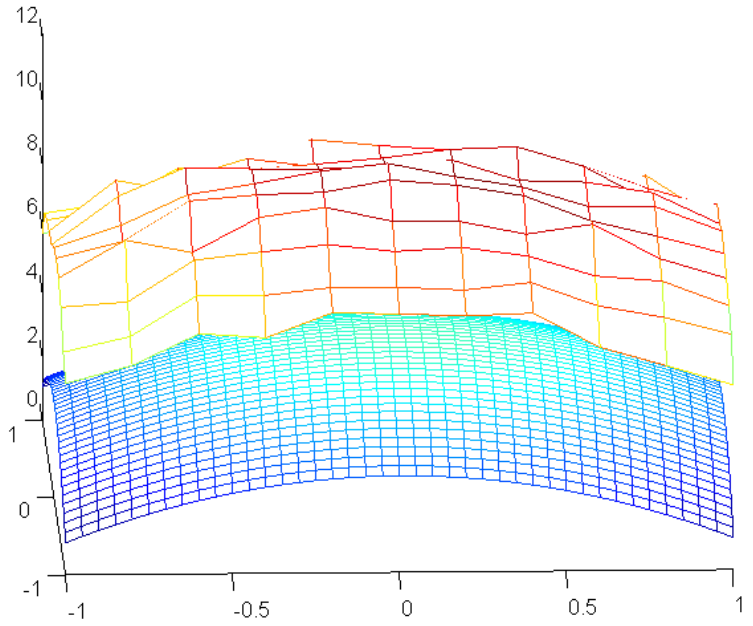


Figure 5.13: Comparison between the approximation $\tilde{a}$ and the exact value $a$ when $k = 100$ in case II.

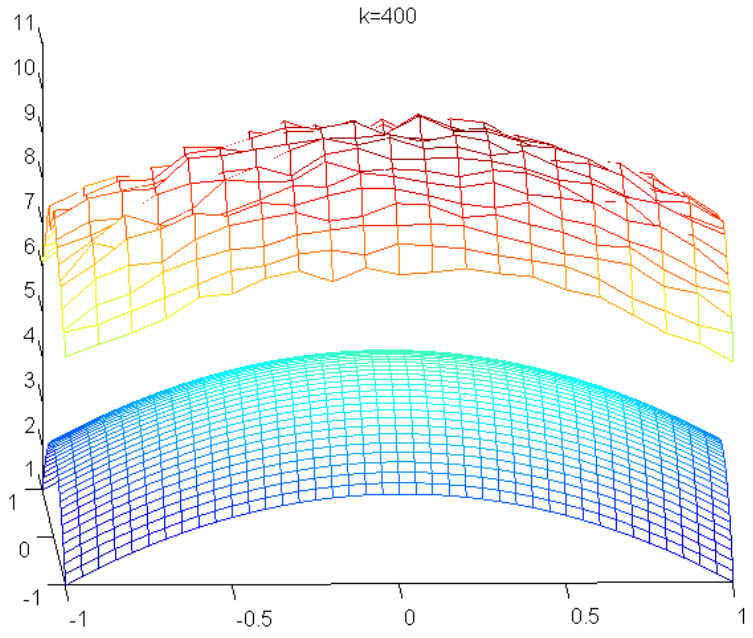


Figure 5.14: Comparison between the approximation $\tilde{a}$ and the exact value $a$ when $k = 300$ in case II.

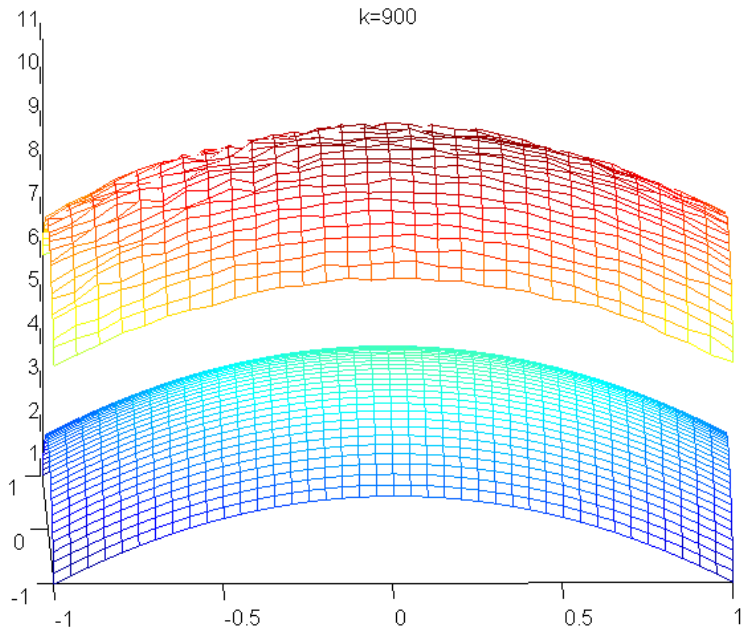


Figure 5.15: Comparison between the approximation $\tilde{a}$ and the exact value $a$ when $k = 500$ in case II.

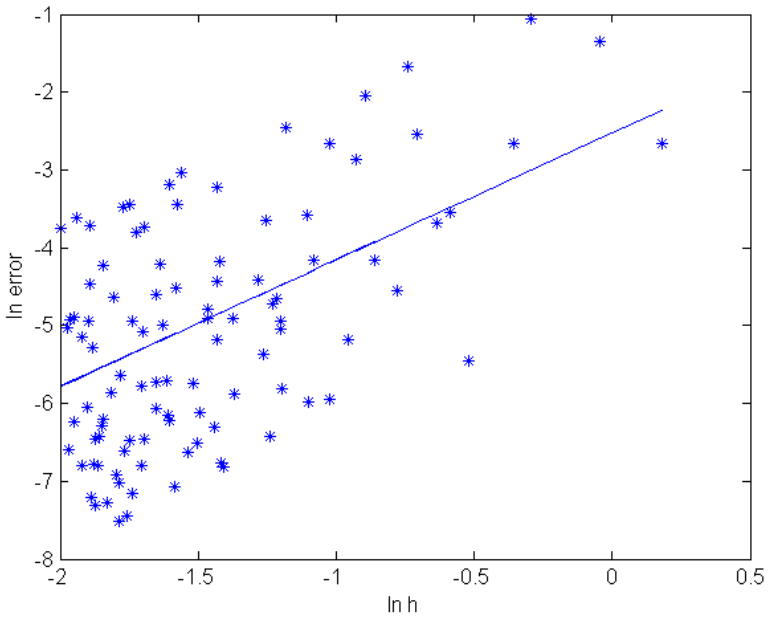


Figure 5.16: Relationship between the average mesh norm $\bar{h}$ and the error estimate $\|\tilde{a} - a\|_{L^\infty}$ in log-log plane in case II. The slope of regression line is 1.633.

Finally, we consider the case when we only have interior data, and no explicit boundary conditions.

## 5.3 Case III: asymptotic boundary condition

This is the most difficult case in that we don't know anything about the boundary, no data information and no location information. We only assume that the following asymptotic boundary condition is satisfied:

$$\lim_{|x|\to\infty} a(x) = 1. \tag{5.6}$$

We can still use RBF methods to reconstruct $\tilde{u}$ and try to reconstruct our coefficient from ODEs. However, the most difficult part is to find the appropriate initial data for our integration. Our aim is to find a new algorithm to solve this problem. The main steps as follows:

(1) Use RBF methods to $\tilde{u}$, $\nabla\tilde{u}$ and $\nabla^2\tilde{u}$.

(2) Set up ODEs to recover $a$.

(3) Guess initial data $a(\tilde{x_0}, y_0)$ for each characteristic curve.

(4) Integrate along each characteristic curve to both directions.

(5) Stop the integration in either direction when $|\nabla^2\tilde{u}| < \epsilon$. We define $\epsilon = 10^{-3}$.

(6) Adjust the boundary data such that the average of $\tilde{a}$ at the endpoints equals the constant 1.

(7) Re-integrate along each characteristic curve using the new initial data.

(8) Invert the mapping and compute the error estimate $\|\tilde{a} - a\|_{L^\infty}$.

We make a slight change to our first example to illustrate our new algorithm. We provide the definition of the exact $a$. However, this time we don't have any information about $\Omega$ and the boundary data on $\Omega$. The only thing we can use in our algorithm is $k$ random interior points.

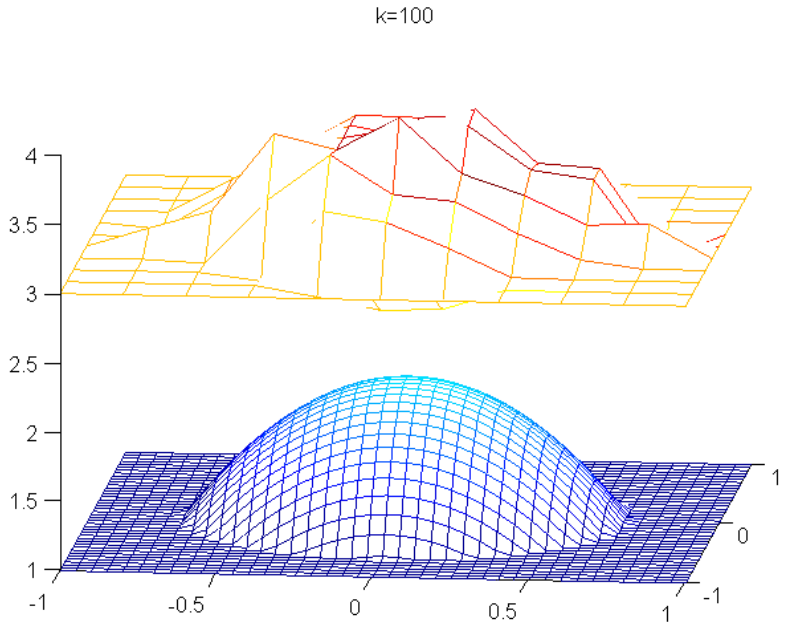


Figure 5.17: Comparison between the approximation $\tilde{a}$ and the exact value $a$, given $k = 100$ randomly chosen interior points.

Let's begin with our test function $a$:

$$a(r) = \begin{cases} 2 - 2|r|^2, & |r| < \sqrt{2}/2, \\ 1, & \text{otherwise.} \end{cases} \tag{5.7}$$

$f(x, y) = 0$. And $u(x, y)$ is the numerical solution of the equation $-\nabla \cdot (a\nabla u) = f$.

The comparison between the exact $a$ and the approximation $\tilde{a}$ of the model problem is shown in Figure 5.17.

Figure $5.17 - 5.19$ indicate that our approximation gets better when we increase the number of interior points. Another thing we deduce from the plots is that the domain of approximation $\tilde{a}$ is larger than the support of $a$. The reason behind this is our new stopping criteria: we stop the integration when $|\nabla^2 \tilde{u}| < \epsilon$. Our next graph

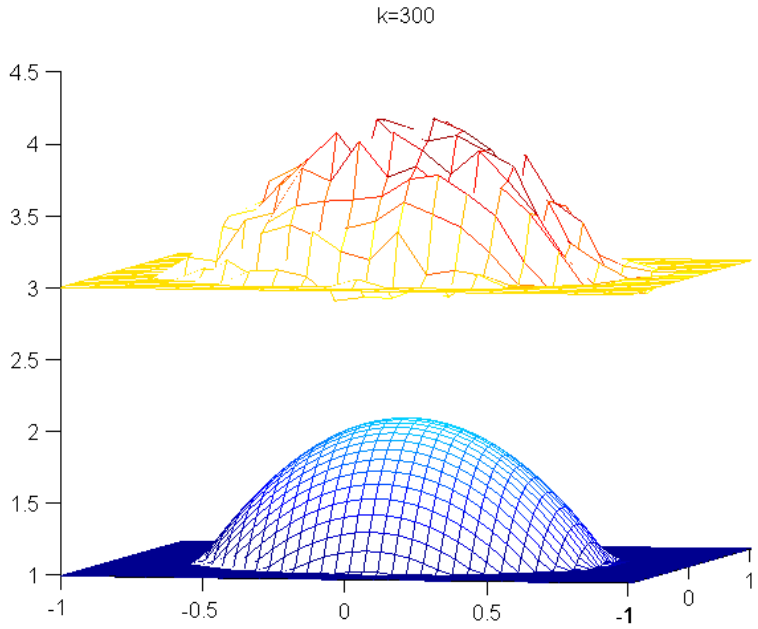


Figure 5.18: Comparison between the approximation $\tilde{a}$ and the exact value $a$, given $k = 300$ randomly chosen interior points.

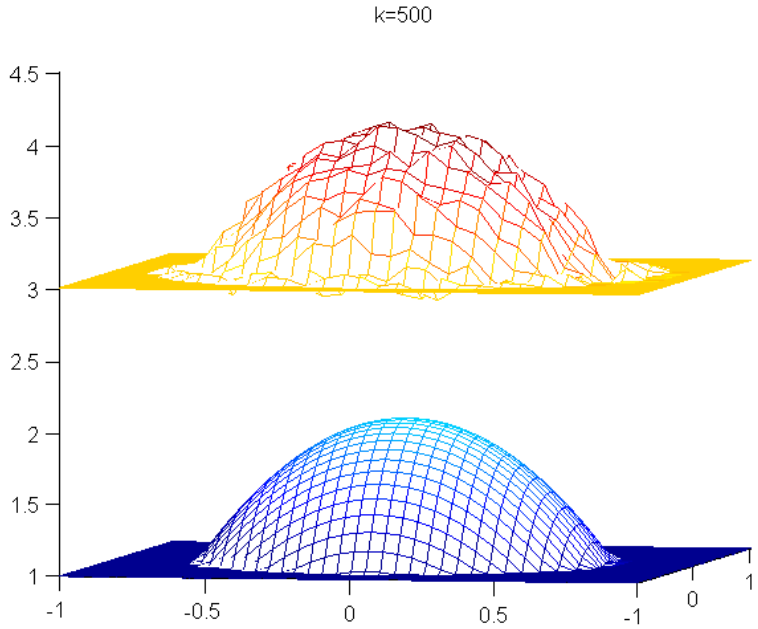


Figure 5.19: Comparison between the approximation $\tilde{a}$ and the exact value $a$, given $k = 500$ randomly chosen interior points.

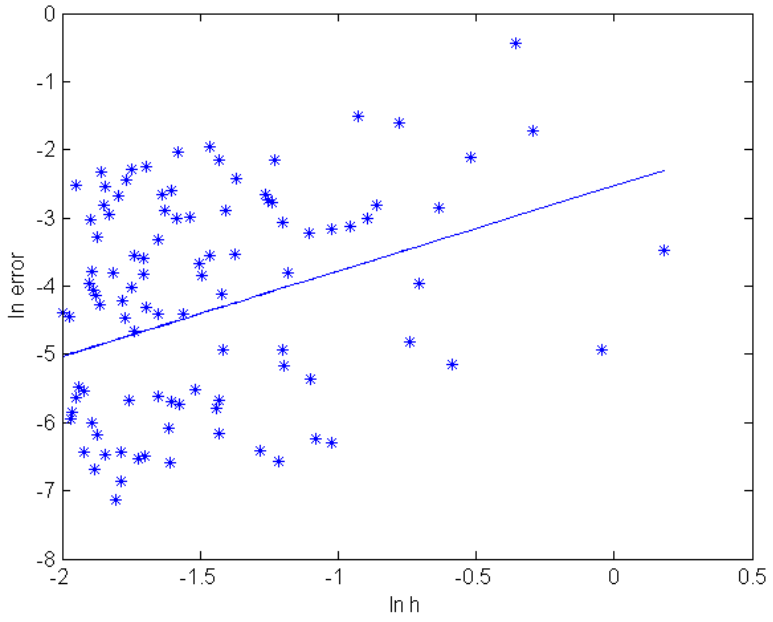


Figure 5.20: Relationship between the average mesh norm $\bar{h}$ and the error estimate $\|\tilde{a} - a\|_{L^\infty}$ in log-log plane in case III. The slope of regression line is 1.175

Figure 5.20 is the logarithmic form of the error estimate we have in this case.

## 5.4 Experimental uncertainty

In this section, we want to discuss the stability of our algorithm under some additional experimental uncertainty, that is observation error. In other words, we assume that our $k$ random interior points satisfy $u(x_i, y_i) = g_i + \psi_i$, $i = 1, 2, ..., k$, where $\psi_i$ is a uniformly distributed random number which satisfies $|\psi_i| < R_1$ for appropriate value of $R_1$. $\psi_i$ simulates "white noise" with amplitude $R_1$.

For convenience, we go back to our first test case in case I and also fix $k = 300$ total random interior points.

For different value of $R_1$, we have series of plots to compare between exact value and approximation value of $a$.

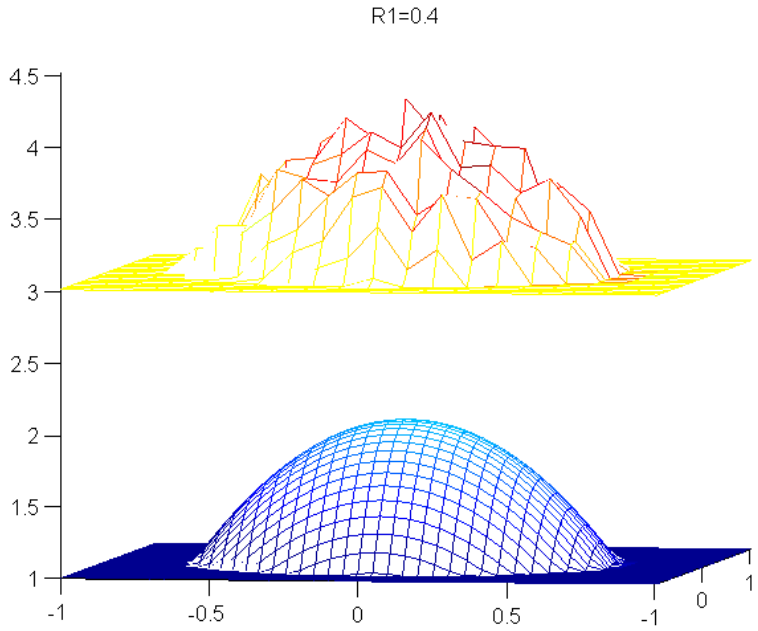


Figure 5.21: Comparison between the approximation $\tilde{a}$ and the exact value $a$ when $R_1 = 0.4$.

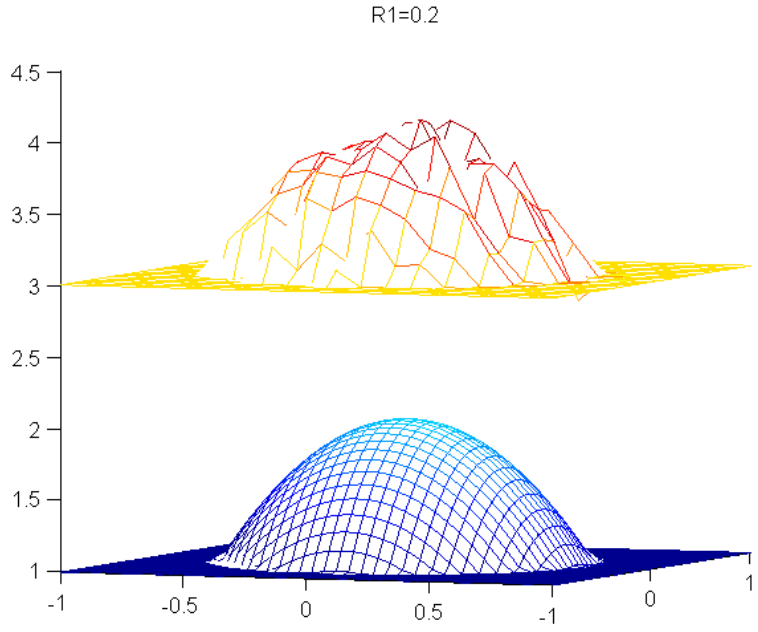


Figure 5.22: Comparison between the approximation $\tilde{a}$ and the exact value $a$ when $R_1 = 0.2$.

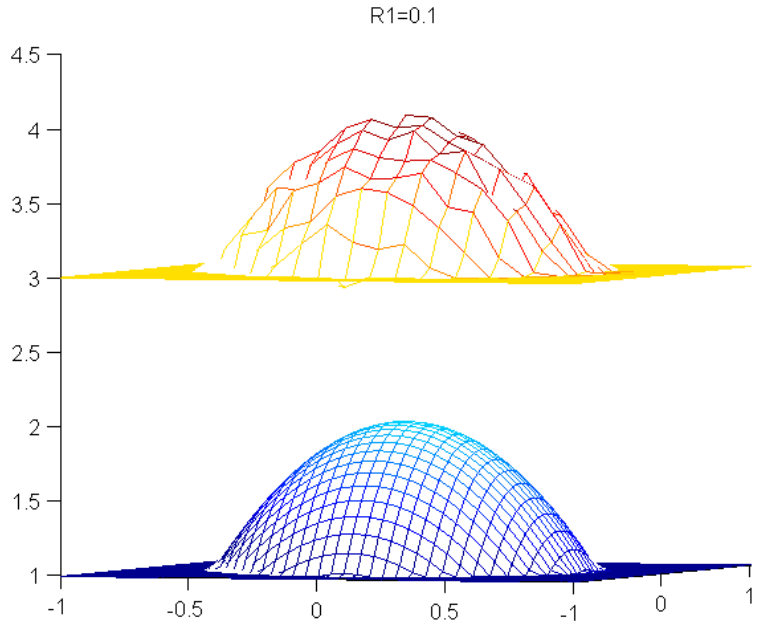


Figure 5.23: Comparison between the approximation $\tilde{a}$ and the exact value $a$ when $R_1 = 0.1$.

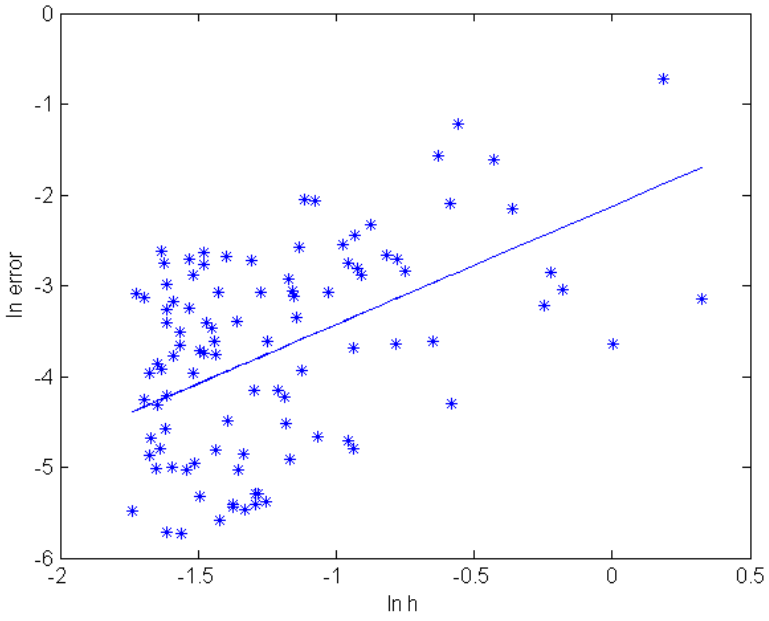


Figure 5.24: Relationship between the average mesh norm $\bar{h}$ and the error estimate $\|\tilde{a} - a\|_{L^\infty}$ in log-log plane in experimental uncertainty. The slope of regression line is 1.303.

## 5.5 Summary

The numerical results in this chapter are summarized in Table 5.1.

| Type of measurements | Boundary condition | $h^r$ |
|---|---|---|
| Uniformly distributed interior points | $a = 1$ on the boundary $\partial\Omega$ | $r = 2.84$ |
| Random subset of uniformly distributed interior points | $a = 1$ on the boundary $\partial\Omega$ | $r = 1.91$ |
| Random interior points | $a = 1$ on non-characteristic curve $\Lambda$ | $r = 1.63$ |
| Random interior points | Asymptotic boundary condition | $r = 1.18$ |

Table 5.1: Summary of the numerical results

After reviewing the figures, we would like to point out three important observations. First of all, the error estimates in each plot, no matter what the boundary condition is or even in the case of no boundary information, decrease when we increase our total number of interior points. In other words, the error decreases when we decrease the value of mesh norm $h$.

Second, and most importantly, the error between exact value $a$ and approximate value $\tilde{a}$ has a linear relationship in the log-log plane. We observe that better boundary conditions in terms of stronger constraints generate better approximation for $a$.

A third note to mention here is that the distribution of inner points also affects our approximation. Uniformly distributed interior points have better approximation than random interior points. Performing multiple simulations with random interior points

and then using the average value of the approximations reduces the uncertainty.

# 6. CONCLUSIONS

We have shown that one can recover the exact value of the parameter $a$ uniquely from (6.1) if $u$ is completely known in a region $\Omega$ with $a = 1$ on the non-characteristic boundary.

We also showed that one can find an approximation $\tilde{a}$ for the unknown parameter $a$ in the elliptic equation:

$$\nabla \cdot (a \nabla u) = f \tag{6.1}$$

from finite data:

$$u(x_i, y_i) = g_i, i = 1, 2, ...k$$

with error estimate:

$$\|a - \tilde{a}\|_{L^\infty} \leq C h^{\tau - 4} (\|u\|_{W^{\tau,2}(\Omega)}),\ \tau > 4 \tag{6.2}$$

under certain smoothness assumptions.

The space $W^{\tau,2}(\Omega)$, $\tau > 4$ appears to be "optimal" since for any weaker Sobolev space ($W^{\tau,2}(\Omega)$, $\tau \leq 4$), $\nabla^2 u$ is not necessarily Lipschitz continuous, and the characteristic system of ODEs (2.36) may not have a unique solution.

If we know a priori information on the boundary of a region (Case I), along a non-characteristic curve (Case II) or using asymptotic boundary condition (Case III), we have found the numerical order of approximation with respect to the mesh norm $h$. Numerical results show that better boundary condition (more constraints) give us better approximations. The numerical algorithm also works when exact value $a$ is close to a piecewise continuous function, in other words, it requires less continuity of $a$ than theory demands.

We have also demonstrated that the errors bounding the numerical reconstructions are consistent with the theoretical error estimates.

# REFERENCES


[1] R.A. Adams and J.J.F. Fournier. *Sobolev Spaces*. Academic Press, New York, NY, 1975.

[2] G. Alessandrini. Stable determination of conductivity by boundary measurements. *Appl. Anal*, 27(1-3):153-172, 1988.

[3] G. Alessandrini. Singular solutions of elliptic equations and the determination of conductivity by boundary measurements. *J. Diff. Eq*, 84:252-273, 1990.

[4] K. Astala and L. Päivärint. Calderón's inverse conductivity problem in plane. *Ann. Of Math*, 163(2):265-299, 2006.

[5] M. Bonnet and A. Constantinescu. Inverse problems in elasticity. *Inverse Problems*, 21(2):R1, 2005.

[6] S. Brenner and L. Scott. *The Mathematical Theory of Finite Element Methods*. Springer, New York, NY, 1994.

[7] A.P. Calderón. On an inverse boundary value problem. *Seminar on Numerical Analysis and its Applications to Continuum Physics*, Rio de Janeiro, 65-83, 1980.

[8] T. Chan and J. Shen. *Image processing and analysis: variational, PDE, wavelet, and stochastic methods*. SIAM, Philadelphia, PA, 2005.

[9] C. Chauvière, J.S. Hesthaven, and L. Lurati. Computational modeling of uncertainty in time-domain electromagnetics. *SIAM J. Sci. Comput*, 28(2):751-775, 2006.

[10] M. Cheney, D. Isaacson, and J.C. Newell. Electrical impedance tomography. *SIAM Review*, 41(1):85-101, 1999.

[11] R. Cont. Model uncertainty and its impact on the pricing of derivative instruments. *Mathematical Finance*, 16:519-547, 2006.

[12] J. Duchon. Interpolation des fonctions de deux variables suivant le principe de la flexion des plaques minces. *Math. Comp*, 10:5-12, 1976.

[13] J. Duchon. Sur l'erreur d'interpolation des fonctions de plusieurs variables par les $D^m$-splines. *RAIRO Anal Numér*, 12(4):325-334, 1978.

[14] L.C. Evans. *Partial Differential Equations*. American Mathematical Society, Providence, Rhode Island, 1998.

[15] R. Franke. *A Critical Comparison of Some Methods for Interpolation of Scattered Data*. TR NPS-53-79-003, Naval Postgraduate School, Monterey, CA, 1979.

[16] R. Franke. Scattered data interpolation: tests of some methods. *Math. Comp*, 38(157):181-200, 1982.

[17] E. Fuselier, T. Hangelbroek, F.J. Narcowich, J.D. Ward, and G.B. Wright. Localized bases for kernel spaces on the unit sphere. *SIAM J. Numer. Anal*, 51(5):2538-2562, 2013.

[18] E. Fuselier, T. Hangelbroek, F.J. Narcowich, J.D. Ward, and G.B. Wright. Kernel based quadrature on spheres and other homogeneous spaces. *Numerische Mathematik*, 127(1):57-92, 2014.

[19] K. Guo, S. Hu, and X. Sun. Conditionally positive definite functions and Laplace- Stieljes integrals. *J. Approx. Theory*, 74:249-265, 1993.

[20] A. Haar. Die minkowskische geometrie und die ann an stetige funktionen. *Math. Ann*, 78:294-311, 1917.

[21] J. Hadamard. *Lectures on Cauchys problem: In linear partial differential equations*. Yale University Press, New Haven, CT, 1923.

[22] T. Hangelbroek, F.J. Narcowich, X. Sun, and J.D. Ward. Kernel approximation on manifolds II: the $L_\infty$ norm of the $L_2$ projector. *SIAM J. Math. Anal*, 43(2):662-684, 2011.

[23] T. Hangelbroek, F.J. Narcowich, and J.D. Ward. Polyharmonic and related kernels on manifolds: Interpolation and approximation. *Found. Comput. Math*, 12:625-670, 2012.

[24] R.L. Hardy. Multiquadric equations of topography and other irregular surfaces. *Journal of geophysical research*, 76(8):1905-1915, 1971.

[25] R.L. Hardy. Theory and applications of the multiquadric-biharmonic method. *Comput. Math. Appl*, 19(8/9):163-208, 1990.

[26] B. Jin and P. Maass. Sparsity regularization for parameter identification problems. *Inverse Problems*, 28(12):123001, 2012.

[27] R.V. Kohn and M. Vogelius. Determining conductivity by boundary measurements. *Comm. Pure Appl. Math*, 37(3):289-298, 1984.

[28] R.V. Kohn and M. Vogelius. Determining conductivity by boundary measurements II: Interior results. *Comm. Pure Appl. Math*, 38(5):643-667, 1985.

[29] P. Kuchment and L. Kunyansky. 2D and 3D reconstructions in acousto-electric tomography. *Inverse Problems*, 27:055013, 2011.

[30] P. Kuchment and D. Steinhauer. Stabilizing inverse problems by internal data. *Inverse Problems*, (28)8:4007, 2012.

[31] C.A. Micchelli. Interpolation of scattered data: Distance matrices and conditionally positive functions. *Constr. Approx*, 2:11-22, 1986.

[32] A.I. Nachman. Global uniqueness for a two-dimensional inverse boundary value problem. *Ann. of Math*, 143(1):71-96, 1996.

[33] F.J. Narcowich and J.D. Ward. Scattered-data interpolation on $R^n$: Error estimates for radial basis and band-limited functions. *SIAM J. Math. Anal*, 36:284-300, 2004.

[34] F.J. Narcowich, J.D. Ward, and H. Wendland. Sobolev bounds on functions with scattered zeros, with applications to radial basis function surface fitting. *Math. Comp*, 74:743-763, 2005.

[35] F.J. Narcowich, J.D. Ward, and H. Wendland. Sobolev error estimates and a Bernstein inequality for scattered data interpolation via radial basis functions. *Constr. Approx*, 24(2):175-186, 2006.

[36] E.D. Nezza, G. Palatucci, and E. Valdinoci. Hitchhikers guide to the fractional Sobolev spaces. *Bull. Sci. Math*, 136:521-573, 2012.

[37] K. Persson and G. Destouni. Propagation of water pollution uncertainty and risk from the subsurface to the surface water system of a catchment. *Journal of Hydrology*, 377:434-444, 2009.

[38] S. Poroseva, J. Letschert, and M.Y. Hussaini. Uncertainty quantification in hurricane path forecasts using evidence theory. *APS Meeting Abstracts*, B1+, 2005.

[39] M.J.D. Powell. The theory of radial basis function approximation. *Advances in Numerical Analysis II: Wavelets, Subdivision Algorithms and Radial Functions*, 105-210, Oxford University Press, Oxford, 1990.

[40] M.J.D. Powell. The uniform convergence of thin plate spline interpolation in two dimensions. *Numer. Math*, 68:107-128, 1994.

[41] M.S. Roulston, G.E. Bolton, A.N. Kleit, and A.L. Sears-Collins. A laboratory study of the benefits of including uncertainty information in weather forecasts. *Weather and Forecasting*, 21:116, 2006.

[42] I.J. Schoenberg. Metric spaces and completely monotone function. *Annals of Math*, 39:811-841, 1938.

[43] D. Shepard. A two-dimensional interpolation function for irregularly spaced data. *Proceedings of the 1968 23rd ACM national conference*, 517-524, New York, NY, 1968.

[44] G. Uhlmann. Electrical impedance tomography and Calderón's problem. *Inverse Problems*, 25:123011, 2009.

[45] W. Walter. *Ordinary Differential Equations*. Springer-Verlag, New York, NY, 1998.

[46] H. Wendland. Piecewise polynomial, positive definite and compactly supported radial functions of minimal degree. *Adv. Comput. Math*, 4:389-396, 1995.

[47] D.V. Widder. *The Laplace Transform*. Princeton University Press, Princeton, NJ, 1941.